POLITECNICO DI TORINO

Master's Degree in ICT for Smart Societies

Master's Degree Thesis

Microgrids for Radio Access Network Resilience

Supervisors

Prof. Michela MEO

Dr. Greta VALLERO

Candidate

Umberto BROZZO DODA

October 2024

Abstract

The power grid supply is always challenged by external factors that may significantly decrease its ability to be able to provide the amount of energy required, therefore making the system unreliable. Many infrastructure relies on the energy provided by the power grid supply and they may malfunction or stop functioning altogether if the energy provided is insufficient. Among these infrastructures, the ones that are most affected by this behavior are the communication infrastructures. The continuity of the communication services is therefore at risk and new ways to make the system more reliable must be found. A possible solution is to supply them through Renewable Energy Sources (RES), particularly Photovoltaic (PV) panels. Moreover, the new smart grid paradigm may allow the possibility to cluster Base Stations (BSs) in the same Radio Access Network (RAN) in a Micro Grid (MG) to be able to exchange the produced energy provided by the PV panels and maximize the continuity of the service when the power grid is not working, as it happens during Power Grid Outage (PGO). The main purpose of this Thesis is to analyze how different characteristics of this scenario and different strategies implemented to manage the energy produced by the PV panels may change the Quality of Service of the system.

Table of Contents

Acronyms

BS
Base Station

DER
Distributed Energy Resources

MG
Micro Grid

PG
Power Grid

PGO
Power Grid Outage

PV
Photovolatic

QoS
Quality of Service

RAN
Radio Area Network

RES
Renewable Energy Sources

TRX
Transceiver

Chapter 1

Introduction

In the last few years, the amount of radio traffic generated by our devices has exponentially increased, as shown in [1], where the data reported from the last ten years shows that mobile data traffic has increased almost 300 times from 2011 to 2021. To be able to face these changes, a reliable infrastructure is required. One of the main causes of disservice is the amount of service outages in the communication network.

As explained in the annual telecom security incidents report provided by ENISA in 2021, [2], the number of incidents affecting the telecom has increased from 2010 to 2021.

ENISA also provides a tool to visualize data regarding incident reports. This tool, called CIRAS [3], can be used to obtain statistics about incidents' cause, their severity, and which technical assets were affected during the incidents.

As shown in Fig.1.1, the number of incidents in 2023 is more than twice the number in 2012. It is also important to notice that, in the last few years, the number of incidents has been stable with a mean of 187 incidents per year.

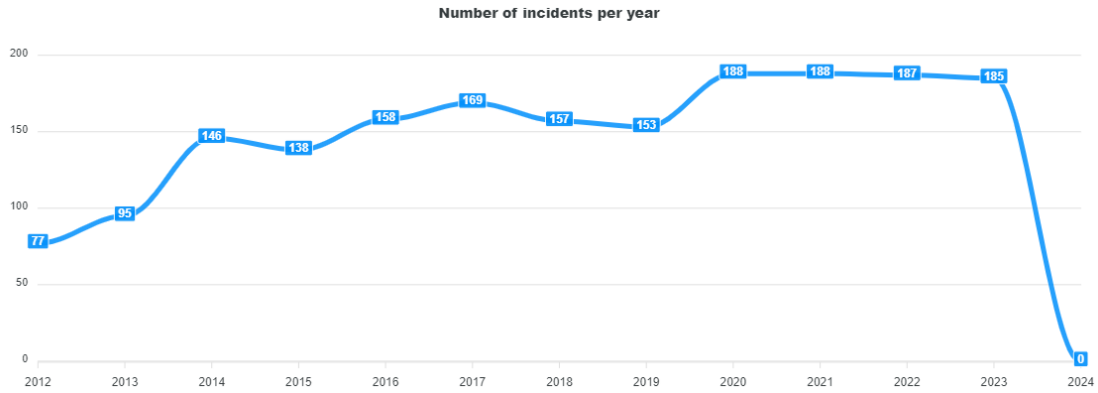

Figure 1.1: Number of incidents reported per year in the telecom

In Fig.1.2 the classification of those incidents by severity is reported. It shows how the number of incidents with a very large impact has been decreasing since 2017 but those incidents are still the most frequent.

Both Fig.1.1 and 1.2 report no data for the current year, this is probably due to the fact that reports of the incidents have not been submitted yet.

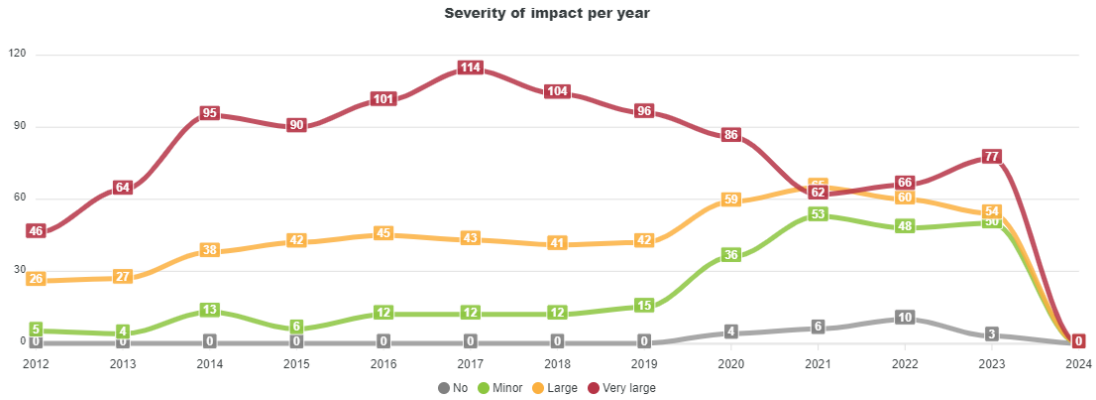

Figure 1.2: Classification of incidents by severity

In order to understand the entity of the incidents, the number of lost user hours from 2012 to 2021 has been reported in Fig.1.3, showing a drastic increase in 2021 with respect to any other year.

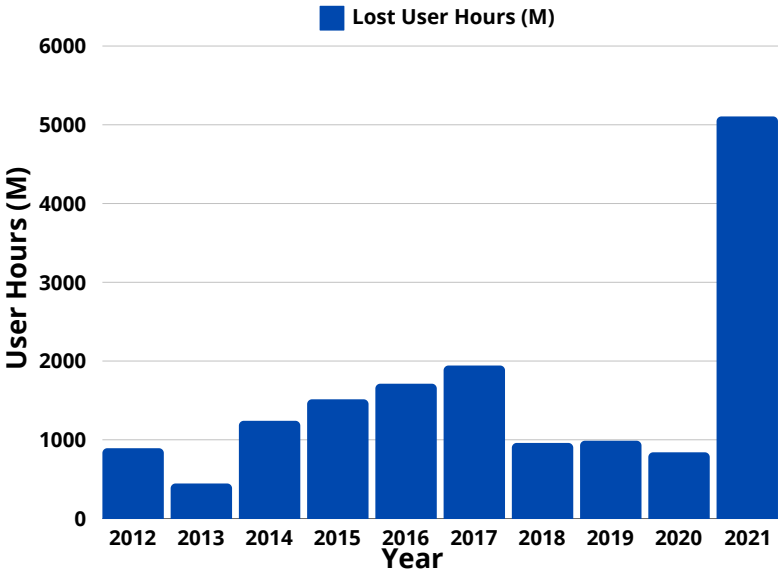

Figure 1.3: Number lost user hours reported per year in the telecom, as reported in [2]

Looking at the technical assets affected by the incidents in the telecom in 2023 reported in Fig.1.4, it is clear that mobile base stations are among the most affected systems, being affected by 23% of the occurred incidents.

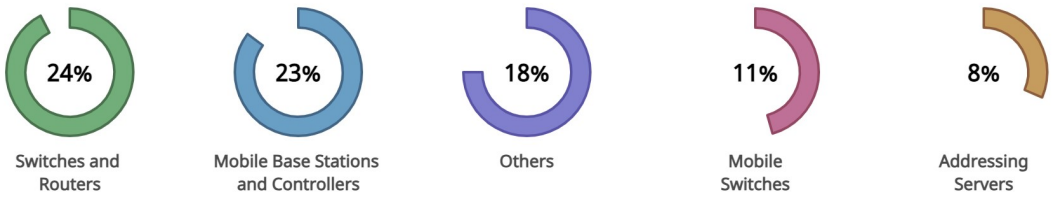

Figure 1.4: Technical assets affected by incidents in 2023, data taken from [2]

In this scenario, reliability is not enough for the system. A RAN, in order to provide a useful service to the users, must be resilient, where resilience can be defined as «the ability to recover from or adjust easily to an unanticipated accident or change», [4]. Considering the RAN scenario, the ability of the network to continue providing service even during a PGO, which is an unanticipated accident, would be considered a great improvement in terms of resilience.

As proposed in [5], the building of a resilient system is composed of three phases, summarized in 1.5, which are:

- Preparedness: the preventive analysis of the system and its surroundings in order to assess which technology best suits the desired purpose and their implementation;

- Response and Relief: the operation of the system under natural hazards that disturb the normal behavior of the system;

- Recovery and Reconstruction: the return to normal behavior of the system that requires finding suitable emergency solutions to be implemented to recover.

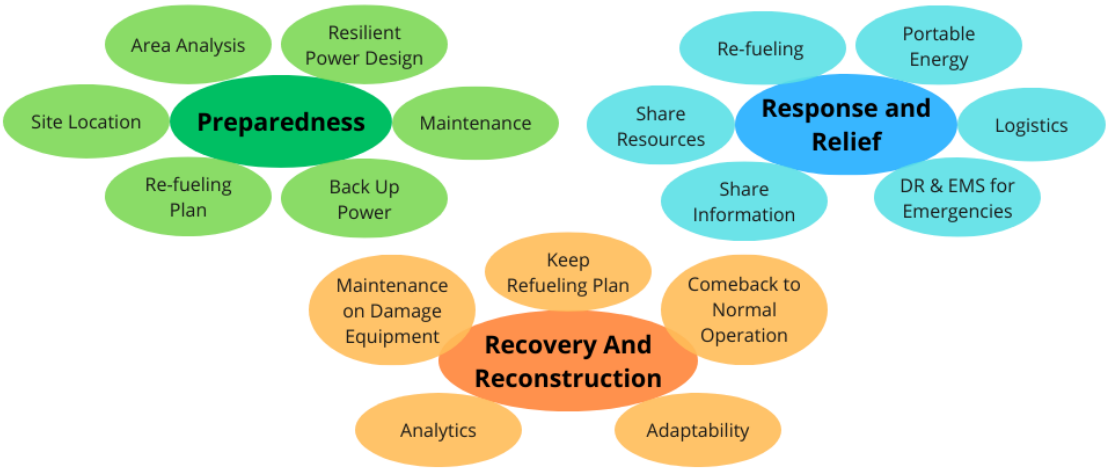

Figure 1.5: Phases to build a resilient system, as stated in [5]

This study will mainly focus on the Response and Relief phase, considering how the RAN responds to the PGOs, but will also partially cover the Preparedness phase, evaluating which technologies such as batteries and PV panels must be implemented beforehand in order to overcome the system disturb.

Since during a PGO, the power grid provides no energy, a way to power the BSs is required. An emerging solution to overcome this problem is the usage of RESs placed in proximity to the stations.

Considering the results shown in [6], it is clear that the safest way to produce energy using RES, and also one of the cleanest, is through the use of PV panels in order to exploit solar energy.

Another important technology that can be used to enhance the resilience of the system is the microgrid. As highlighted in [7], MGs are useful technologies that can be used to improve the resilience of the system with respect to the available energy.

MGs are becoming very popular nowadays thanks to their flexibility and the capacity to be easily controlled,[8].

An MG, to function, requires an energy supply, which, in the considered case, would be provided by PV panels, and an appropriate energy management algorithm to optimize the distribution of the available energy throughout the grid. The latter will be one of the main focus of this analysis.

The usage of these technologies in telecommunications has already been proposed in [5], where the main solutions to improve the resilience of the network are proposed. Also, the main topologies to implement an MG are proposed and they will be analyzed in sec.2.

1.1 Thesis objective

This thesis aims at studying how a system combining these two technologies would perform. The system is composed of multiple BSs that manage a variable amount of traffic depending on the hour of the day and the month. Each BS is equipped with PV panels that provide an energy supply. The BSs are grouped in clusters and the BS in each cluster are connected to one another in an MG in order to exchange energy. The considered structure is reported in Fig.1.6.

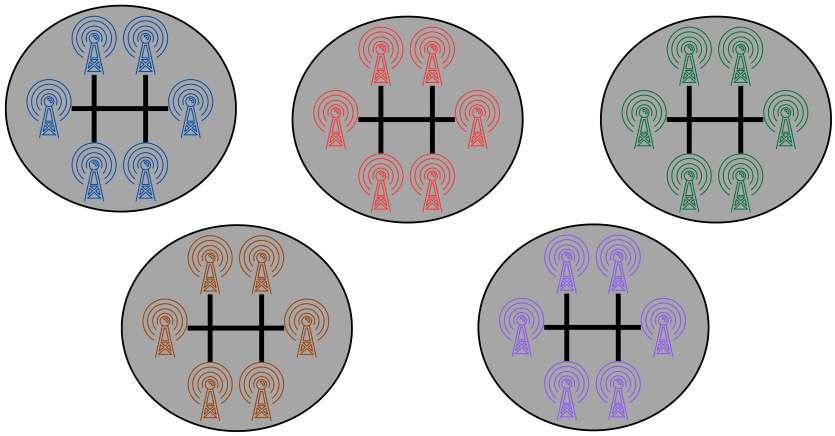

Figure 1.6: Example of a Radio Area Network composed by BSs arranged in MGs

Since the main focus of this work is on the resilience of the system, only the times in which anomalous conditions are present are studied. In the case study, the considered anomalous condition is the one in which a Power Grid Outage occurs. During a PGO, the MG can only rely on the energy coming from the PV panels.

This study will focus on how different aspects of the configuration of the system will impact its performance and on how it will perform in different conditions.

The main aspects that will be analyzed will be:

- Different energy management system;
- Usage of batteries;
- Microgrid topology.

The different conditions under which the system will be studied are:

- Different months of the year;
- Different hours of the day, in particular considering hours in which daylight allows for the PV panels to produce energy;

- Presence of losses in the links between BSs.

The main indicator that will be studied to evaluate the performance of the system will be the percentage of traffic that the system can manage under the studied conditions.

The Thesis is organized as follow:

- Sec.2 review related work analyzing the main technologies used in this work and their implementation;
- Sec.3 explains which scenarios have been studied and reports the results obtained in each of them;
- In Sec.4 the results are discussed in order to determine if technologies under study may increase the QoS provided by the system.

Chapter 2

State of the Art

The State of the Art will focus on the main technologies and paradigms that will be deployed in this work. The main aspects to be studied are the following:

- The usage of Microgrid and the modality of their implementation with a focus on how they can improve the resilience of a system also using Renewable Energy Sources.
- The modelization of a Base Station to calculate its energy consumption based on the amount of traffic it is managing.
- The modelization of a PV panels to calculate their energy production.

2.1 Microgrids

As stated by the Conseil International des Grandes Réseaux Électriques (CIGRÉ) Working Group C6.22 Microgrid Evolution Roadmap (WG6.22), Microgrids are "*electricity distribution systems containing loads and distributed energy resources, (such as distributed generators, storage devices, or controllable loads) that can be operated in a controlled, coordinated way either while connected to the main power network or while islanded*".

In [9], the main qualifiers for a Microgrid are defined. *Generators* can be any energy source within the MG, covering both fossil and renewable. *Storage devices* enclose all types of energy storage, e.g. electrical, electrochemical, and mechanical, therefore they also include batteries. *Controlled loads* refers to all those loads in the MG whose energy consumption can be modulated, giving more flexibility to the system in terms of overall energy requirements.

Another important aspect that is taken into account in the paper is the fact that an MG can operate either while connected to the Grid or in an islanded

configuration. In the former case, the MG is able to collect energy from the Power Grid in case the production within the MG itself is not enough to cope with the consumption of the system. In the latter, the MG only relies on its generators and storage devices. In this case, the presence of controlled loads become more important as it allows for the system to modulate its energy consumption based on the available energy.

Considering the definition given for an MG, it's possible to define the main components present in our case study. The Pv panels represents the generators and they are the only energy source in the system. The controlled loads are the BSs, that can be turned on and off based on the available production from the PV panels. Also, batteries are present, which are the storage devices, but their usage will be studied only in sec.3.5. The considered MGs are usually connected to the Power Grid, but, since they will be studied under the condition that a PGO is happening, no energy is provided by the Power Grid, so they can be considered islanded.

Considering the algorithm used for optimizing the utilization of the resources produced by the MGs, different algorithms will be studied in sec.3.

In [9], some of the benefits derived from the implementations of an MG are emphasized, in particular, it is stated that MGs can improve system efficiency, reduce emissions, and improve power quality and reliability.

As proposed in [10], DERs play a very important role considering the generator part. The paper also suggests different ways to optimize the utilization of DERs and different algorithms that can be implemented for this purpose.

As supported in [11], MGs provide great flexibility and adaptability, which are the main characteristics required to integrate the usage of RES in a system. The article emphasizes that the usage of RES in MGs can enhance the reliability of the system and improve its energy efficiency.

MGs are particularly interesting as they help to relieve the Power Grid and to increase the resilience of a system when Power Grid Outages occur, as shown in [12], in particular in remote places where a breakdown in the power supplying infrastructure is more difficult to manage. The study also stresses how important they are from an environmental point of view as they help integrate RES into the supply system. Indeed, MGs allow for the usage of both flexible and non-flexible energy sources, the latter usually requiring storage systems which are crucial to compensate for the fact that energy coming from RES is not reliable, like in the case of PV panels producing only during the day and whose production depends on the amount of available daylight.

The unreliability of the energy sources is one of the main issues that is under study about MGs, as it leads to a decrease in the voltage of the system and to a deviation of the frequency from its nominal value, as stated in [13]. Therefore, studying how to make energy production more reliable is crucial in order to

improve the system. A possible solution is proposed in [14], where a self-triggering mechanism to overcome the problem is proposed.

In [15], where a review of the main solutions to reduce the problem of unreliability of RES is proposed, it is stressed how the main factor that can relieve the system from this problem is, again, an Energy Storage System. Another proposed solution is the usage of complementary RES, i.e. using multiple RES which are expected to produce in different moments, in order to balance one another.

A very crucial point to overcome the fluctuation in energy production is the implementation of an Energy Management System, as in [16]. This system should be able to analyze data coming from the MG, forecast the load and production, and optimize the utilization of energy. Another important aspect of the system is that it should provide a human interface for the interaction between the MG's operators and the MG itself.

Figure 2.1: Comparison of energy produced by photovoltaic and onshore wind, data taken from [17]

Focusing on the RES used in the MG, in many cases in the literature PV panels have been used to supply the system. Examples of studies in which MGs are powered using Photovoltaic can be found in [18], [19], and [20]. In particular, [18] focuses on the usage of strategies to control the photovoltaic inverters and ensure the correct output voltage is provided to the system, which is again one of the main issues to be solved in an MG system as said previously, in [19] a consumption model of a photovoltaic MG is proposed based on Genetic Wavelet Neural Network, and [20] focuses again on the stability of the MGs from the voltage point of view.

The large usage of Photovoltaic among all other renewable is supported by the fact that solar energy is expected to lead a transition towards renewable, along with wind energy, as explained in [21], an article proposed by the International Renewable

Energy Agency (IRENA) on the expected results to be obtained using solar energy. In [22], data are proposed comparing the current and the expected situation in the future of the utilization of renewable. From 2010 to 2029 the production of solar energy has increased almost seven-fold, whereas energy generated from the wind only doubled. By 2050, solar energy is expected to provide 360 GW/year, compared with 240 GW/year coming from wind energy.

Moreover, data from [17] shows the energy produced by different RES. In Fig.2.1, data for the energy produced using photovoltaic and onshore wind have been reported showing an increase in the energy produced by PV panels from 2018.

2.2 Base Stations consumption model

As stated in [23], finding a way to correlate the amount of traffic managed by a BS and the energy required by the BS to operate is a crucial point in the telecom. The paper proposes a case study in Ghana and is based on a model of power consumption based on two components: one traffic-dependent and one traffic-independent. Then these two components can be divided into other components considering which elements in the BS consume energy based on the amount of traffic and which do not. The traffic-independent considered components were the Bas Band Unit (BBU), the EMUA, the Air Conditioning modules, the Incandescent Bulbs, and the Rectifier. The only traffic-dependent component considered is the power consumed by the Radio Unit. The parameters of a model for the traffic-dependent component are then estimated using a simple linear regression. The proposed model is the following:

$$p = \alpha_0 + t\alpha_1 + \varepsilon \tag{2.1}$$

Where p is the power consumed, t is the traffic managed, ε is a random noise with zero mean, and α_0 and α_1 are the parameters of the model.

Another model is proposed in [24]. Starting from the BS scheme present in Fig.2.2, were the structure of a transceivers (TRX) is reported, the energy consumption of the BS is calculated as the consumption of a TRX multiplied by the number of antennas in the BS (considering that each antenna requires a single TRX).

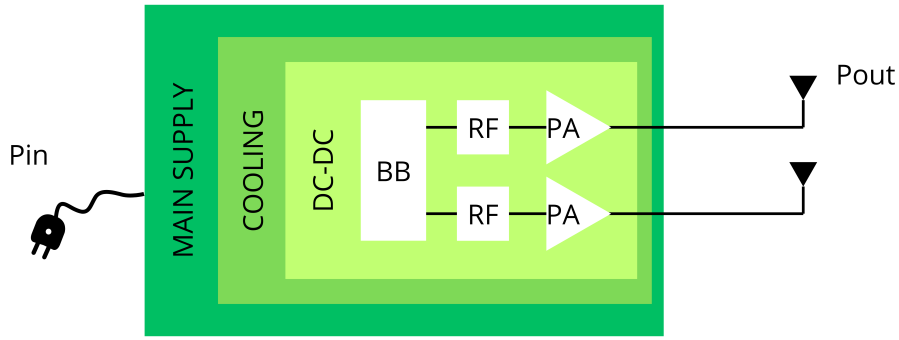

Figure 2.2: BS main part scheme

Considering the Power Amplifier, its energy consumption when the efficiency is η_{PA}, and the output power is P_{OUT}, is equal to:

$$P_{PA} = \frac{P_{OUT}}{\eta_{PA}(1 - \sigma_{feed})} \tag{2.2}$$

where σ_{feed} is a factor to take into account the loss given by the distance between the BS and the antenna, which are usually not in the same place in macro BS.

At this point it is possible to evaluate the energy consumed by the BS considering the case in which the number of TRX is N_{TRX}, and with a power consumption of the Base Band Unit P_{BB} and of the Radio Frequency small-signal Unit P_{RF}, as:

$$P = N_{TRX} \frac{\frac{P_{OUT}}{\eta_{PA}(1-\sigma_{feed})} + P_{RF} + P_{BB}}{(1 - \sigma_{DC})(1 - \sigma_{MS})(1 - \sigma_{cool})} \tag{2.3}$$

where σMS, $\sigma cool$, and σDC are the losses due respectively to the main supply,to the cooling system, and to the DC-DC power supply.

From this, a linear model is derived. Considering the energy consumed by the BS when in sleep mode P_{sleep}, and the minimum non-zero output power P_0, the consumption is eqaul to:

$$P = \begin{cases} N_{TRX} P_0 + \Delta_p P_{out} & 0 < P_{out} \leq P_{max} \\ N_{TRX} P_{sleep} & P_{out} = 0 \end{cases} \tag{2.4}$$

where Δ_p is a parameter that must be estimated from data and correlates the consumption with the output power.

Another possible way to get the consumption of a BS is to use black box models like Artificial Neural Network, as done in [25]. In particular, a multilayer perceptron has been used, composed of fully connected layers. The goal was to estimate the consumption of BSs, but, since it was expected that some parameters regarding the system might not be taken into account, some errors in the estimation were expected. To overcome this problem, the data collected to train the model were considered noisy, and the mean and standard deviation of the energy consumption were estimated. The input layer, composed of 84 neurons, was used to input data regarding both the type of antennas used in the BS and the amount of traffic managed by the antennas. Than two fully connected were implemented, one with 40 neurons, and the other with 15 (the values were find after an optimization part). Finally, an output layer was implemented, using neurons with a sigmoid function. The model was trained using an ad hoc loss function and data from 7500 BSs'antennas. Considering the obtained results, the model had very good performance, especially considering the MAPE which was lower than 6%.

In [26], a similar model has been used. In this case, the total power consumption is modeled using the following equation:

$$p = N_a(P_t + P_{dsp} + \nu P_a) + P_r + P_c + P_{bh} \tag{2.5}$$

Where all the elements are reported in Table 2.1, with the value to be used for the considered case study.

Table 2.1: 5G consumption model parameters

Parameters	Description	Values
P_t	Power required by the TRX	100W
P_{DSP}	Power required by the Digital Signal Processor	100W
N_a	Number of antennas	1
P_{bh}	BH power link	10W
ν	Efficiency of the amplifier	0.5
P_c	Cooling system	200W
P_r	Rectifier power	50W

Since this model is more flexible and allows changing the parameters with ones more suited for the considered case study, this model has been used in this work.

2.3 PV panels production model

A platform implementing a model for the PV panels production is already implemented at [27].

The platform allows for the calculation of the amount of energy produced by a set of PV panels based on different parameters, giving an hourly estimation based on a typical meteorological year.

The model takes different parameters to take into account the characteristics of the considered system of PV panels. The main ones used for the case study are reported in table 2.2 with the value used.

Table 2.2: PV panels production parameters

Parameters	Values
Technology	crystalline silicon
System Size	4kW
System Losses	14%
DC/AC Inverter Efficiency	96%
Tilt Angle	20°
Azimuth Angle	180°
Location	Milan

The platform calculate the energy production using the following procedure, explained in [28]:

1. Given surface tilt β, surface azimuth γ, solar azimuth γ_{sun}, and solar zenith θ_{sun} angles, otained either by the input parameters or by the Solar Resource, calculate the Angle Of Incidence α:

$$\alpha = cos^{-1}[sin(\theta_{sun})cos(\gamma - \gamma_{sun})sin(\beta) + cos(\theta_{sun})cos(\beta)] \tag{2.6}$$

2. Calculate the beam of Irrdainace as the beam normal input multiplied by the cosine of α.

3. Calculate the Plane-Of-Array Irradiance summing the beam componenet with the ground-reflected diffuse one and the sky diffuesd one, calculated using the Prez model as in [29]:

$$I_{poa} = I_b + I_{d,sky} + I_{d,ground} \tag{2.7}$$

4. Calculate τ_{cover}, the transmittance through the cover of the PV panels in order to get the transmitted POA irradiance I_{tr}.

5. Calculate the temperature of the cell, T_{cell}, as in [30].

6. Compute the loss factor:

$$L(\%) = 100(1 - \prod_i (1 - \frac{L_i}{100}) \tag{2.8}$$

7. Compute the DC power as follow:

$$P_{dc} = \frac{T_{tr}}{1000} P_{dc0}(1 + \nu(T_{cell} - T_{ref}))(1 - \frac{L}{100}) \tag{2.9}$$

where ν is the coefficient that correlate the difference of temperature with respect to a reference point T_{ref} and the efficiency of the panel, and P_{dc0} is the nameplate DC rating.

8. Considering the inverter model with nominal efficiency η_{nom} and real efficiency η, calculate the DC power:

$$P_{ac} = \begin{cases} \eta P_{dc} & 0 < P_{dc} < P_{dc0} \\ P_{dc0}\eta_{nom} & P_{dc} > P_{dc0} \\ 0 & P_{dc} = 0 \end{cases} \tag{2.10}$$

Chapter 3

Methodology

To analyze the scenario proposed in Sec.1, a RAN in Milan has been considered. The network is composed of 1418 BSs. The scope is to analyze how this RAN would perform during a PGO if MGs were created to connect the BSs.

Each considered BS uses a 5G technology and it works at a frequency of 2.1 GHz using a channel with a bandwidth of a maximum 120 MHz.

In order to simulate the behavior of the BSs during PGO, a framework has been created, that simulates what happens to the RAN during the PGO. Each simulation considers multiple MGs (i.e. cluster of BSs) and multiple PGOs. Each simulation is done with a one-minute granularity.

At each time step of the simulation, three main variables regarding each BS must be taken into account:

- Production: the amount of power produced in a BS by PV panels placed in proximity of the BS itself. The data regarding the PV panels production were collected using the PVWATT tool [27], whose characteristics are explained in [28]. Thanks to this tool, it is possible to gather information about the production of PV panels in Milan. The energy produced in the i-th BS at time t will be referred to as $P_i^{(t)}$.

- Traffic: the amount of traffic that is injected into each BS. The data relating to the traffic were provided by an Italian Mobile Network Operator and refered to a two-month time period in 2015. In order to be compliant with the increasing traffic demand in the considered region from the time of the collection of the data to 2024, the data were scaled according to [31]. The factor used is equal to 7.5. The amount of traffic injected into the i-th BS at time t will be referred to as $T_i^{(t)}$.

- Consumption: the amount of power required by the BS to remain active and provide service for all the injected traffic. In order to obtain this amount, a

model of the energy consumption of a BS is required. The model employed in this study is the one proposed in [32]. Given the number of elements of the BS antenna N_a, the power required by the transceiver in Watt P_t, the power required by the Digital Signal Processor P_{dsp} the efficiency of the amplifier ν, and the power injected into it P_a and considering the power required by those elements whose number does not depend on the number of antennas in the BS, which are the rectifier consuming P_r, the cooling system consuming P_c and the backhaul link consuming P_{bl}, the energy consumed by the BS i-th BS in the MG at time t can be expressed as:

$$E_i^{(t)} = t(N_a(P_t + P_{dsp} + \nu P_a) + P_r + P_c + P_{bh}) \tag{3.1}$$

As said before, the used framework allows a muli-MG and multi-PGO simulation with one-minute granularity. In order to do this, the simulator requires three types of information:

- Traffic load of each BS: as said before, this has been provided by an Italian Mobile Network Operator. The data refers to a two-month period in 2015 and reports the hourly load of about 1400 BSs with a 15-minute granularity. The considered BSs are situated in Milan and its surroundings. Since data from two months are provided, the average daily pattern has been computed. In order to be compliant with the framework, the granularity has been changed from 15 minutes to 1 minute. To do this, at first data were aggregated to get an hourly granularity. Then the values are linearly interpolated and divided by 60 to get a granularity of one minute.

- Production of PV panels: as said before, data were obtained through the PVWATT tool. The tool allows to get data regarding the PV panels production in the considered area, and it also takes into account the main losses the main losses the system is subjected to. The obtained data are at hourly intervals and correspond to a whole year. Data were later scaled to obtain a one-minute granularity required by the framework.

- PGO time of occurrences and duration: the information regarding the PGO was collected in [33] using an API that was provided by a Distribution System Operator. For each outage, it is recorded the month in which it happens, the hour of the day, and its duration. Since in many cases having outages of different durations can be misleading and the duration of an outage can affect the obtained results, files containing information about synthetic outages have been created and used during the simulations. Synthetic outages are outages with a fixed duration of one hour, occurring during the same month and each at a different our of the day, one for each our of a considered time period. Since

during the PGO the only source of energy are the PV panels, it makes sense to considered PGOs that happend during the daytime, therefore the considered time period goes from 8 A.M. to 8 P.M. with the last outage starting at 7.00 P.M. and ending at 7.59 P.M. for a total of 12 outages in each file. This also means that, when using a synthetic PGOs file in the framework, each MG will simulate 12 different outages.

The main idea of the used process is to start from a simple configuration of the MG, from now on referred to as default configuration, and compare the results obtained with this configuration with those obtained by making changes to it.

The default configuration has the following characteristics:

- BSs are divided into clusters with the same cardinality, N. In this study, two different values of N will be used, $N = 3$ and $N = 8$. The division is done by putting together BSs with similar characteristics for the incoming traffic (i.e. the clusters are homogeneous). In order to do this, a K-means approach has been employed.
- Each BS has a PV panel. All the PV panels generate the same amount of power (i.e. $P^{(t)_i}$ is the same for all the BS in the RAN and it only depends on the month and hour of the outage, and the time t).
- The BSs are placed in an MG with a fully mashed topology, which means that all the BSs in the same MG are connected to one another and can directly exchange energy without the need to send the energy to an intermediate node.
- The connections between BSs are made so that there is no loss during the exchange of energy.
- Each BS can be in either one of two states: on, which means the BS is working and all the traffic injected is managed, or off, which means that no traffic is managed. It is possible to define a variable $s_i^{(t)}$ which indicates the state of the BS i at time t and which is equal to 1 if the state is on and 0 if it is off. The energy consumed by the BS can be expressed as:

$$C_i^{(t)} = E_i^{(t)} s_i^{(t)} = \begin{cases} E_i^{(t)} & \text{if } i\text{-th BS is on,} \\ 0 & \text{if } i\text{-th BS is off} \end{cases} \tag{3.2}$$

- Each MG has the same resource management strategy to decide, in case the production of all the PV panels in the MG is not enough to maintain all the BSs on, which BSs should be turned off. The strategy implemented is straightforward: in case the production is not sufficient, the BSs should be turned off in increasing order of traffic. The flowchart of the strategy is

reported in Fig.3.1. At the beginning, all BSs in the MG are considered active and the production and consumption of the whole MG are calculated. At this point, if the consumption is greater than the production, the active BS with the lowest traffic is turned off. The procedure is repeated until the production is greater or equal to the consumption.

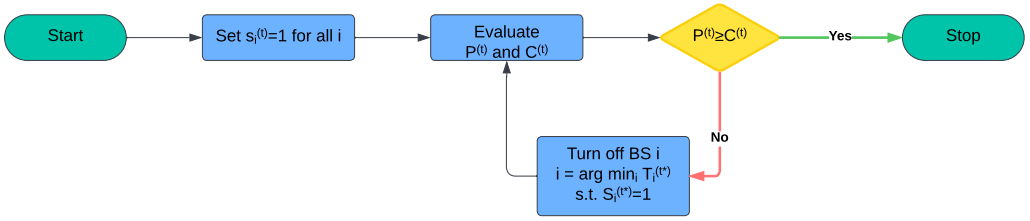

Figure 3.1: Flowchart of the behavior of the MG

In this case, two more variables were defined as follow:

$$P^{(t)} = \sum_{i=1}^{N} P_i^{(t)} \tag{3.3}$$

$$C^{(t)} = \sum_{i=1}^{N} C_i^{(t)} = \sum_{i=1}^{N} E_i^{(t)} s_i^{(t)} \tag{3.4}$$

3.1 Comparing traffic characteristics and performance in different months

Before starting the analysis described in sec.1, it can be useful to analyze the characteristics of the default configuration. To do this, true outages were used considering one outage for each hour (in the considered time range) in each month. A total of 144 outages were simulated for each MG in the RAN. This procedure has been applied both when $N = 8$ and $N = 3$.

Fig.3.2a shows the average rate of traffic incoming in each BS at each hour of the day and how it changes in different months. As it is possible to notice, the traffic is increasing during the day but is pretty much constant during the year. Fig.3.2b shows the percentage of managed traffic during each PGO. It is easy to deduce that in the summer period (June, July, and August) when daylight is present for longer periods, the percentage of managed traffic starts increasing earlier in the day and stays higher during the evening. Moreover, since the solar radiation is higher, the percentage of managed traffic is higher as more energy is

produced. During the winter period (November, December, and January), the opposite behavior can be seen: the curve representing the percentage of managed traffic starts increasing later in the day and rapidly decreases again and it reaches a lower value at peak hours. Fig.3.2c instead shows, for each month, the maximum percentage of managed traffic during a PGO. As said before, the value is lower in the winter period and higher in the summer period.

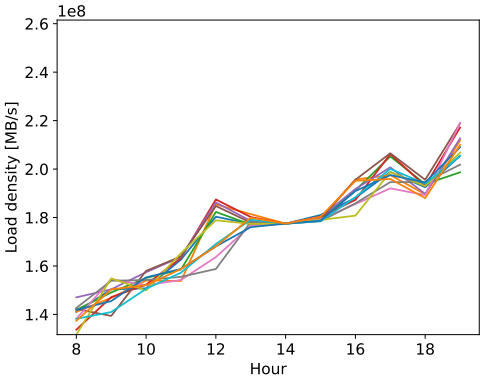

(a) Density of incoming traffic

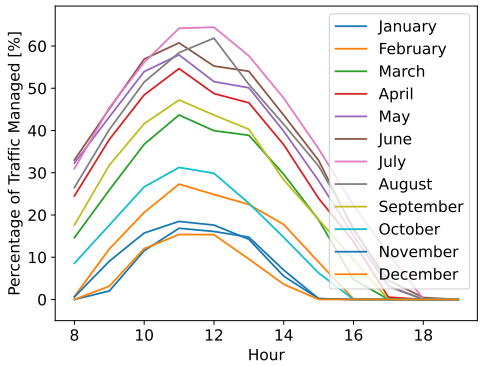

(b) Percentage of traffic managed

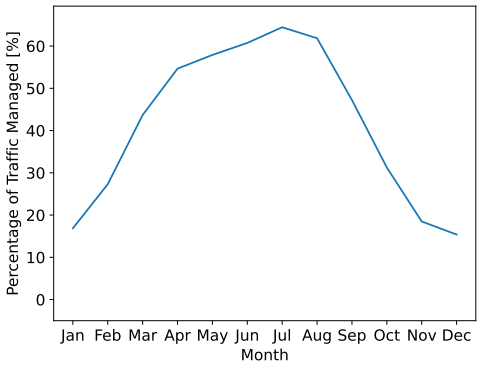

(c) Maximum percentage of traffic managed per month

Figure 3.2: Results of the simulation done with the default configuration when each MG contains 8 BS

Figures 3.3a, 3.3b, and 3.3c show the same results for MGs containing 3 BSs. The results show the same behavior seen with the MGs with 8 BSs.

Considering how the month in which the PGO happens affects the data, it is possible to define a best-case scenario and a worst-case scenario. So, in the next parts of the analysis, two months will be considered: July and December.

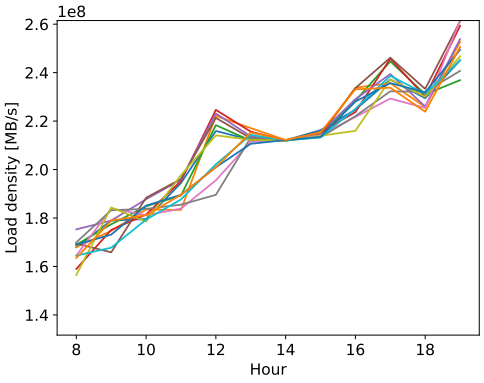

(a) Density of incoming traffic

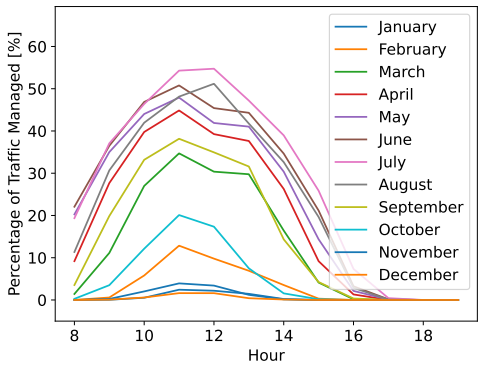

(b) Percentage of traffic managed

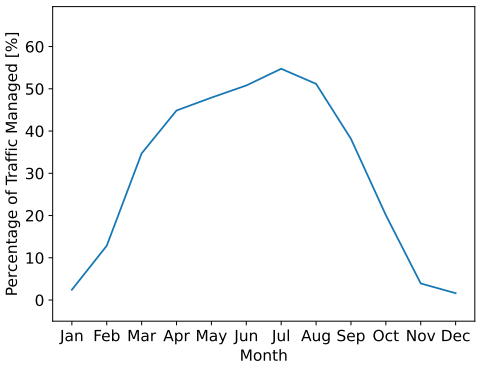

(c) Maximum percentage of traffic managed per month

Figure 3.3: Results of the simulation done with the default configuration when each MG contains 3 BS

3.2 Comparing different strategies to decide where to allocate energy available in the MG

It is now possible to start making changes to the default configuration. The first thing we will analyze is how the control strategy for the management of resources in the MG affects the performance.

The simple control logic proposed in sec.3 has two main characteristics: it is memoryless (so the choice at $t-1$ does not affect the choice at t) and greedy, based on the assumption that maintaining active fewer BSs with higher traffic is better than having more BSs with lower traffic.

Considering these characteristics, two possible changes can be made:

- Introducing memory with respect to the choice of active BSs made in the previous timeslot.
- Inverting the order in which the BSs are turned off by favoring the ones with lower traffic in order to be able to increase the number of active stations.

The latter change can be easily summarized by the flow chart in Fig.3.4.

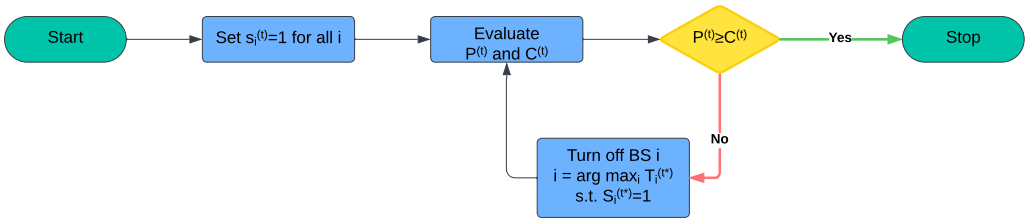

Figure 3.4: Flowchart of the behavior of the MG, favoring BSs with lower traffic

The implementation of a simple control logic implementing memory is shown in Fig.3.5. At first, the consumption in case all the BSs in the MG are active is evaluated. If the production is not sufficient, all the BSs are set to the state that they had at $t-1$. With this state, the consumption is again computed. At this point, three cases are possible:

- If the new consumption is equal to the production, the algorithm stops.
- If the consumption is higher than the production, the algorithm starts turning off the BSs with lower traffic until the consumption drops below the production.
- If the consumption is lower than the production, a function σ is defined. The function, given a value j between 1 and N, returns the index of the j-th BS with the lowest traffic. At this point the algorithm tries iteratively to activate a new BS starting from the ones with the highest traffic. The algorithm stops when all the BS have been evaluated.

In this case, priority is given again to BSs with higher traffic. In fact, when we want to turn off a BS we select the active one with the lowest traffic, and when there is an exceeding part of production we try turning on BSs starting from the one with the highest traffic.

It is also possible to invert the priority order giving higher importance to the BSs with lower traffic. In this case, when we want to turn off a BS we select the active one with the highest traffic, and when there is an exceeding part of production

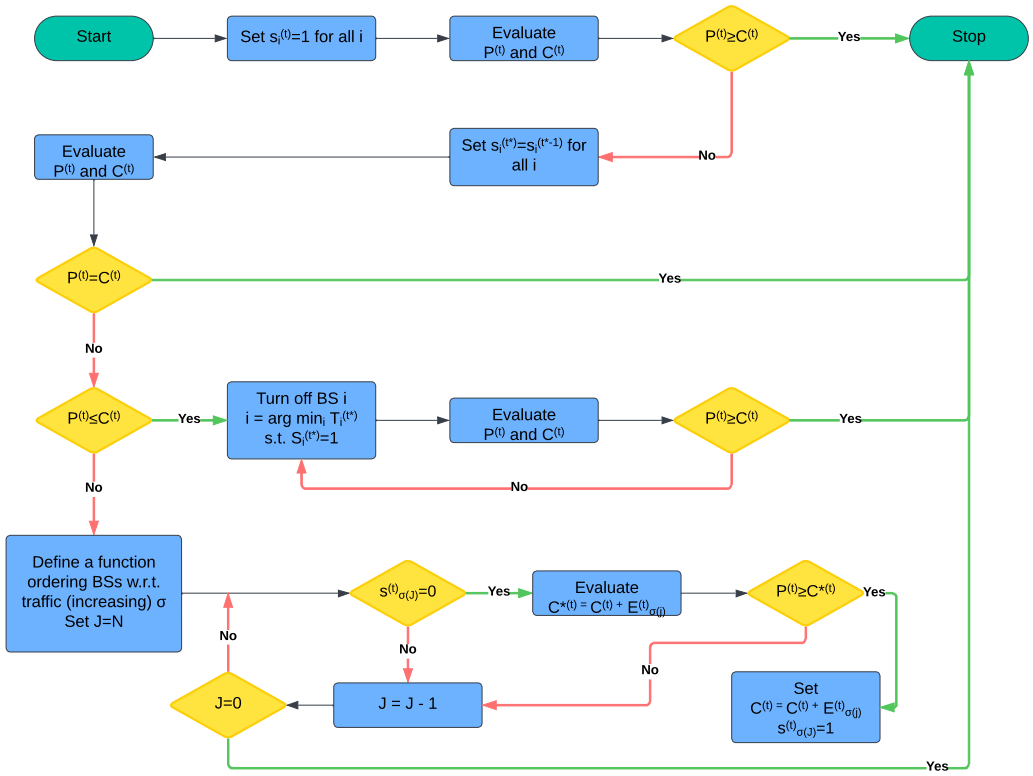

Figure 3.5: Flow chart of control logic implementing memory giving priority to BSs with higher traffic

we try turning on BSs starting from the one with the lowest traffic. This logic is applied in the flow chart reported in Fig.3.6.

In the legends of the images, the words "memory" and "memoryless" are used to identify whether the used algorithm implements memory or not, and the terms "Hfirst" and "Lfirst" are used to identify respectively whether higher priority is given to the BSs with lower or higher traffic. Therefore the scenarios that will be analyzed in this part are four:

- memoryless_Lfirst: case in which there is no memory and priority is given to the BS with higher traffic. It is the default configuration.
- memoryless_Hfirst: case in which there is no memory and priority is given to the BS with lower traffic.
- memory_Lfirst: case in which memory is implemented and priority is given to the BS with higher traffic.

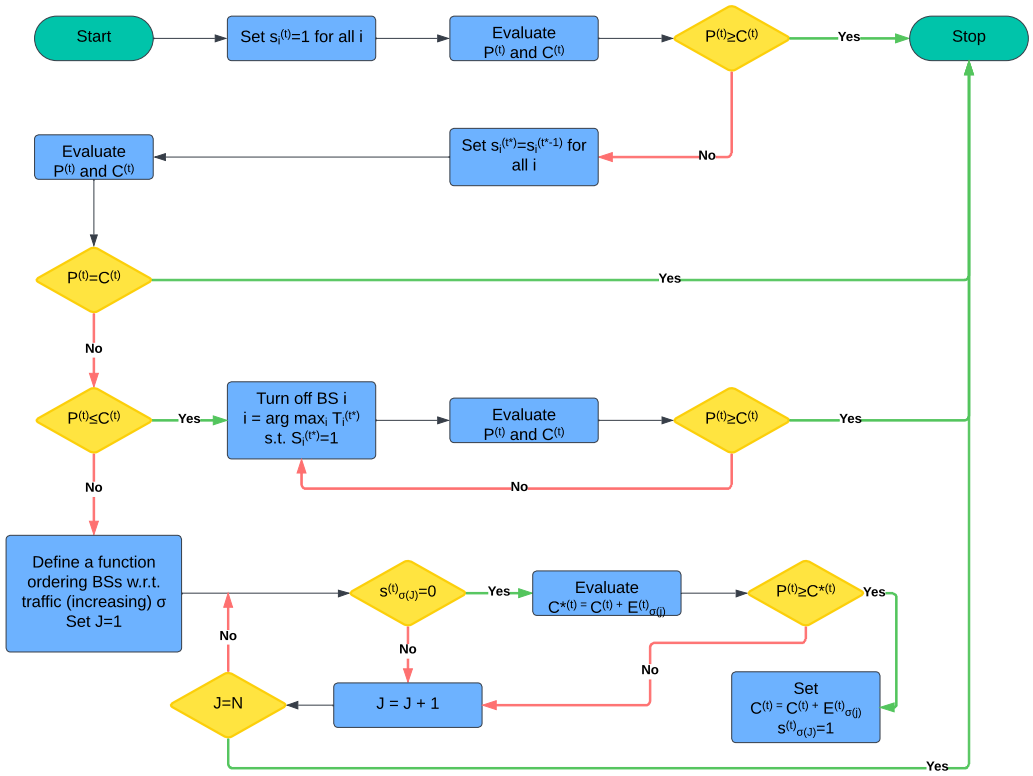

Figure 3.6: Flow chart of control logic implementing memory giving priority to BSs with lower traffic

- memory_Hfirst: case in which memory is implemented and priority is given to the BS with lower traffic.

To evaluate the performance of these four algorithms, they were used in simulations done with MG composed of 3 and 8 BSs (from now on the number of BSs in an MG will be referred to as cardinality), and both in July and December. The PGOs used were synthetic outages as explained at the beginning of Sec.3.

The performance indicators used to assess the results were the following:

- Percentage of managed traffic: it is calculated by computing the traffic managed by an MG during a PGO over the total load injected in the same MG in the same period. In the graph, the average value over all MGs in the RAN is reported. Moreover, the interval between the minimum and maximum values is highlighted.
- Average number of active BSs: it is calculated by averaging the number of

active BSs in an MG over each minute of simulation. As before, in the graph, the average value over all MGs in the RAN is reported and the interval between the minimum and maximum values is highlighted. For this parameter, also a graph of its standard deviation is reported.

- Switch rate: considering an MG, the total number of times any BS changes state (either from on to off or vice versa) is computed and divided by the total simulation time in seconds. As before, in the graph, the average value over all MGs in the RAN is reported and the interval between the minimum and maximum values is highlighted.

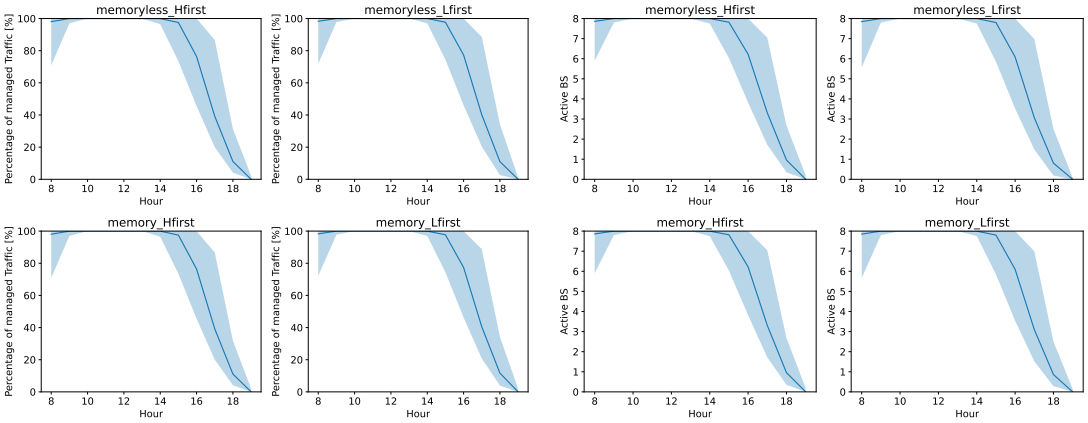

(a) Percentage of managed traffic **(b)** Average number of active BSs

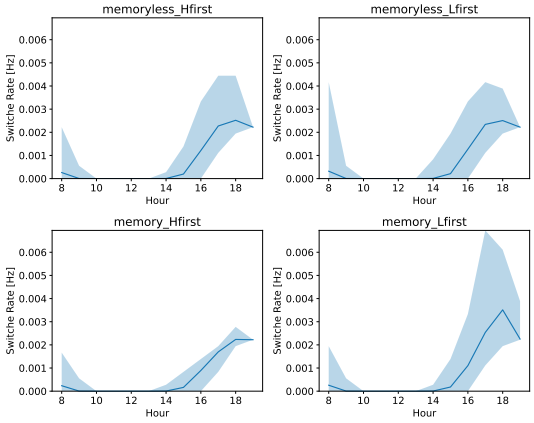

(c) Rate at which the BS switch status

Figure 3.7: Results for Cardinality=8 and outages in July

Starting with the simulations done with MGs composed of 8 BSs and outages happening in July, Fig.3.7a shows the average percentage of traffic managed by all

the MGs in the RAN. It is possible to notice that the highest value is reached at midday when the production is higher.

It is possible to notice that the interval between the maximum and minimum values at peak hour is null and the average value is 100%, which means that in this time period, in July, the produced energy is enough for the whole system to work properly.

Fig.3.7b, shows the average number of active BS in the MGs. This figure shows great similarity with the previous due to the fact that the number of active BSs is strictly correlated with the percentage of managed traffic.

Fig.3.7c reports the switch rate. The best scenario is the one with memory where priority is given to BSs with lower traffic. This is especially evident in the afternoon: in fact, when in the afternoon the production starts decreasing, turning off more loaded BSs allows to maintain the active BSs on for longer. With this configuration, the rate is lower than 0.003 Hz, which means that on average in an MG every 5 minutes one out of eight BSs changes state.

Fig.3.8 instead shows the standard deviation of the average number of active BSs in the MGs. During peak hours the standard deviation is low because the energy is enough for the whole system to work, whereas in the morning and evening, it is still low but for the opposite reason, i.e. there is no energy produced by the PV panels so the whole system is off.

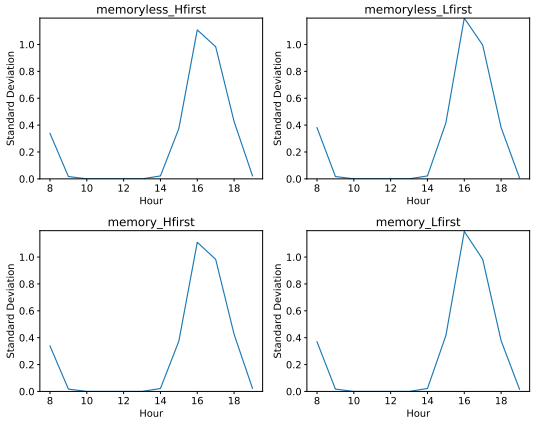

Figure 3.8: Standard deviation of the average number of active BSs in MGs with Cardinality=8

Fig.3.9 shows the same results when the RAN is split in MGs composed of 3 BSs. In general, the behavior is the same, but, considering the interval between the minimum and maximum of the considered parameters, it is possible to notice that the intervals tend to be larger, especially for the switch rate, where the rates are higher. This indicates that MGs with lower cardinality tend to be less stable.

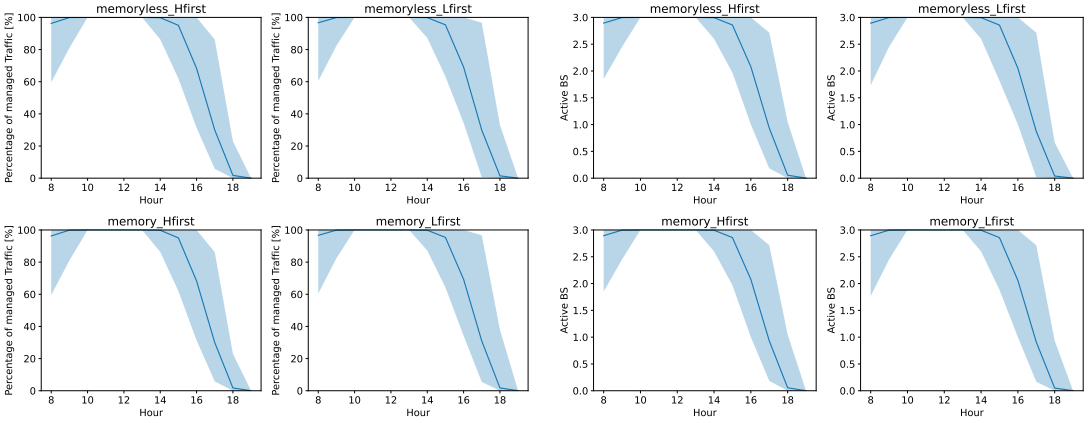

(a) Percentage of managed traffic **(b)** Average number of active BSs

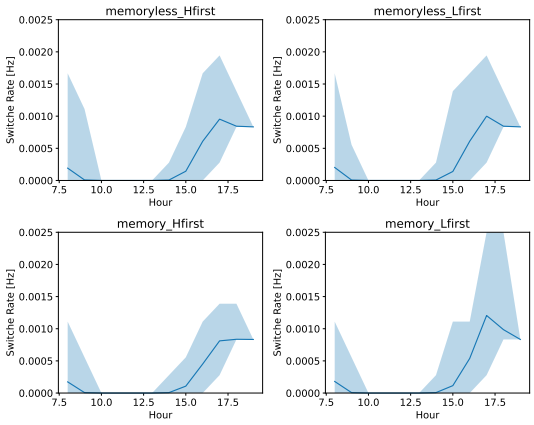

(c) Rate at which the BS switch status

Figure 3.9: Results for Cardinality=3 and outages in July

The standard deviation of the average number of active BSs, reported in Fig.3.10 shows the same behavior as in the previous case.

At this point, the same simulations were done in December. Fig.3.12 shows, for both the case with cardinality equal to 8 and the one with cardinality equal to 3, the percentage of managed traffic, the average number of active BSs, and the switch rate. Differently from the cases in July, in December the production at peak hours is not enough to always guarantee that all the BSs in the RAN can be activated.

Considering the switch rate, in every considered case, after 4 P.M. it is always equal to 0.002Hz if the cardinality is 8 and 0.00075Hz if the cardinality is equal to 3. The expected time between a switch and another is respectively 8 minutes and 22 minutes. Considering a PGO during 60 minutes, this means that in the

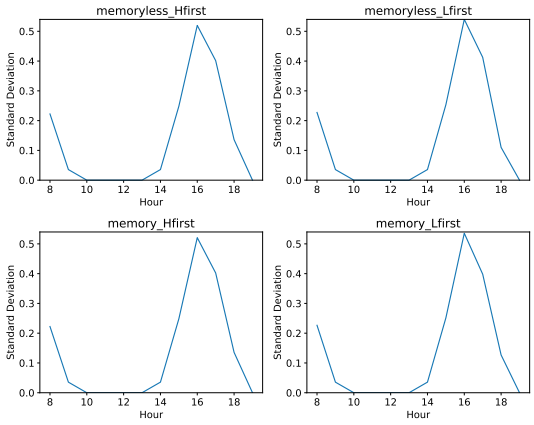

Figure 3.10: Standard deviation of the average number of active BSs in MGs with Cardinality=3

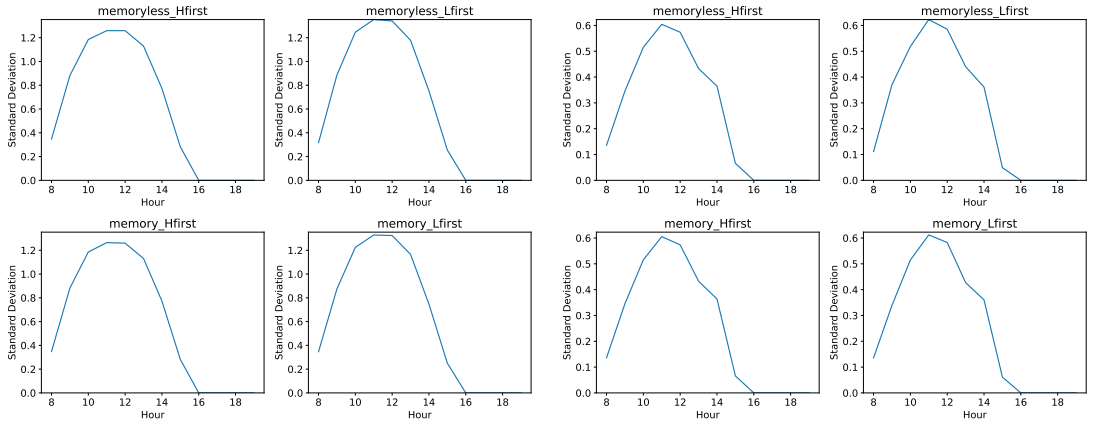

(a) Cardinality=8 **(b)** Cardinality=3

Figure 3.11: Standard deviation of the average number of active BSs for outages in December

first case, there should be 8 switches in total, and in the second 3. The result is equal to the cardinality as in the afternoon the energy becomes so low that no BS manages to stay active, so the switch corresponds to every BS in the MG turning off at the beginning of the PGO.

Fig.3.11 shows the standard deviation of the average number of active BSs in December. It is possible to notice that this value reaches its peak at 12 P.M. due to the fact that at that hour the production is the highest with respect to the rest of the day, but, contrary to what happens in July, the total energy required by the system is still higher.

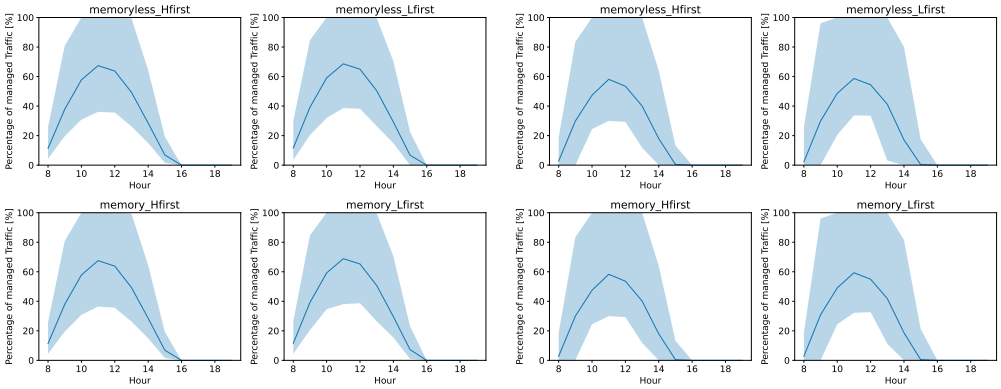

(a) Percentage of managed traffic Cardinality=8

(b) Percentage of managed traffic Cardinality=3

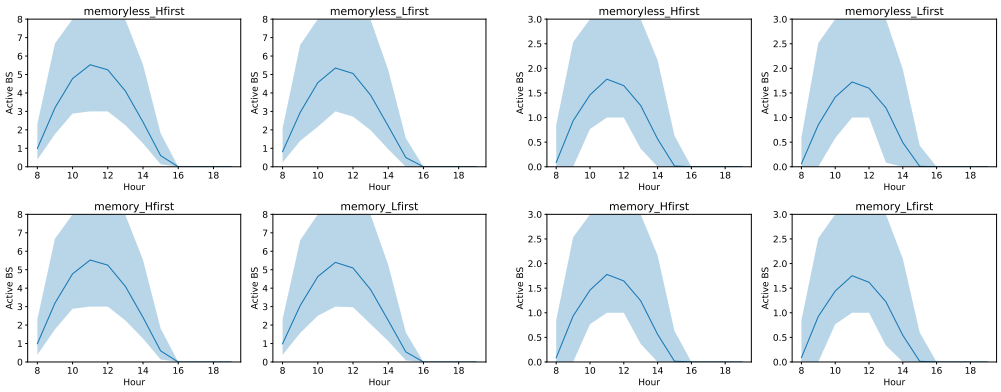

(c) Average number of active BSs Cardinality=8

(d) Average number of active BSs Cardinality=3

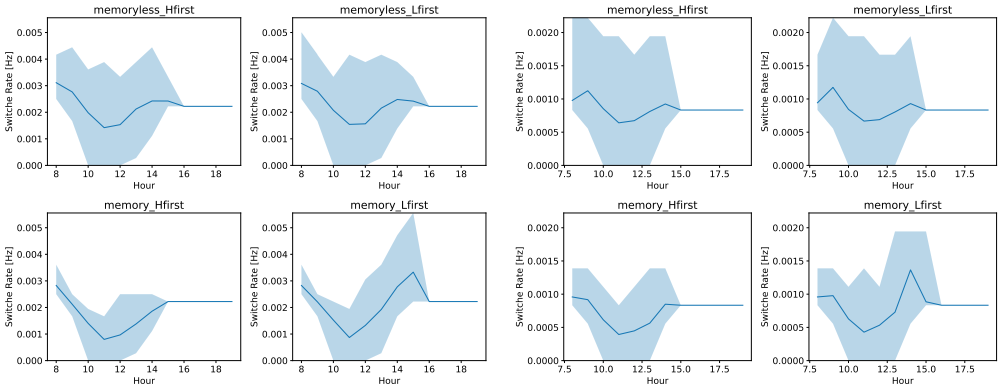

(e) Rate at which the BS switch status-Cardinality=8

(f) Rate at which the BS switch status Cardinality=3

Figure 3.12: Results for outages in December

3.3 Analyzing best-performing and worst-performing clusters

From the results obtained in the previous section, it is evident that different clusters perform differently, and this behavior is especially visible at certain hours of the day depending on the month. This is due to the fact that different clusters have different loads, so the energy required by each MG is different.

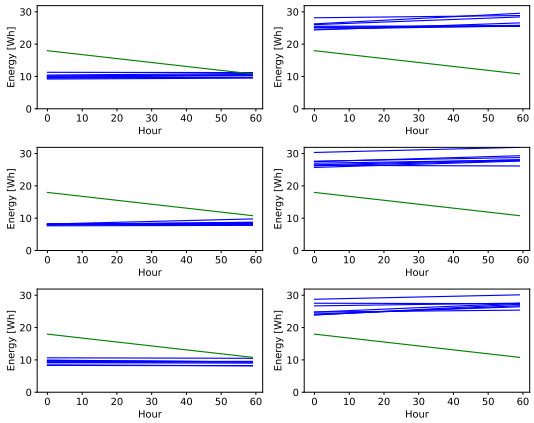

(a) Energy required by each BS with respect to the average production

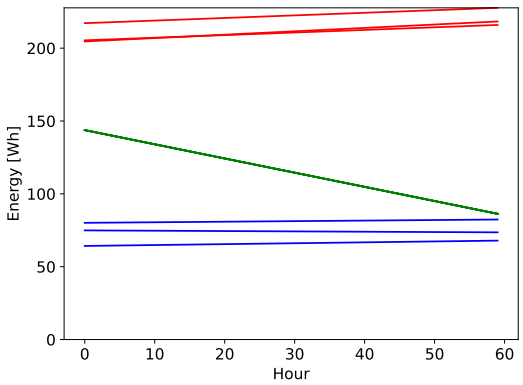

(b) Total consumption of the MGs

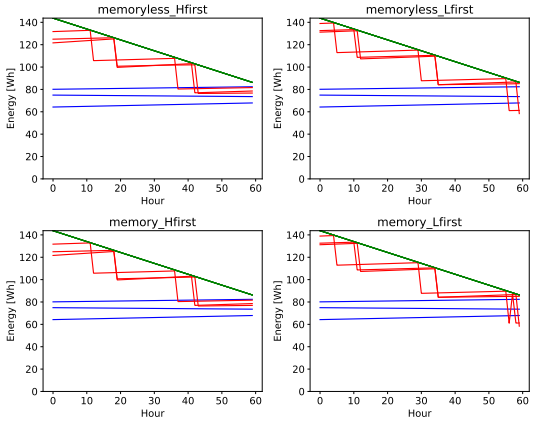

(c) Energy consumed by each observed MG

Figure 3.13: Cluster analysis for Cardinality=8 and outages in July

Given these results, it can be interesting to analyze some clusters to study this behavior. In this section, for each cardinality, the three clusters performing better, and the three performing worst were studied. In order to decide which cluster to analyze, the percentage of managed traffic was considered. The value was taken at

one of the hours of the day when the standard deviation of the average number of active BSs was higher. All the simulations in this section where done using synthetic PGOs during the month of July.

Considering the case with cardinality equal to 8, the studied clusters were chosen considering the results at 4 P.M.

For the six considered clusters, Fig.3.13a shows for each cluster the energy required by each BS in the MG to work during the PGO happening at 4 P.M. In the same figure, also the average production of the BSs in the MG is reported. Considering that the three clusters on the left are the ones chosen as the best, and the ones on the right are chosen as the worst, it is already possible to notice that in the first case, BSs tends to have an energy required which is lower than the average production.

Fig.3.13b shows the total consumption of each observed MG with respect to the production of the whole MG. Since the same production model is used for each PV panel in any BSs, the total energy produced by each BS (and therefore by each MG) is the same. In the image, the green line represents the production, the red lines represent the energy required by the MGs performing poorly, and the blue lines represent the one from those performing the best.

Fig.3.13c shows for each of the four scenarios considered in the previous section, the energy consumed by each MG. It is possible to notice that when the consumption saturates the production, there is a drop in the consumption itself as a BS is turned off.

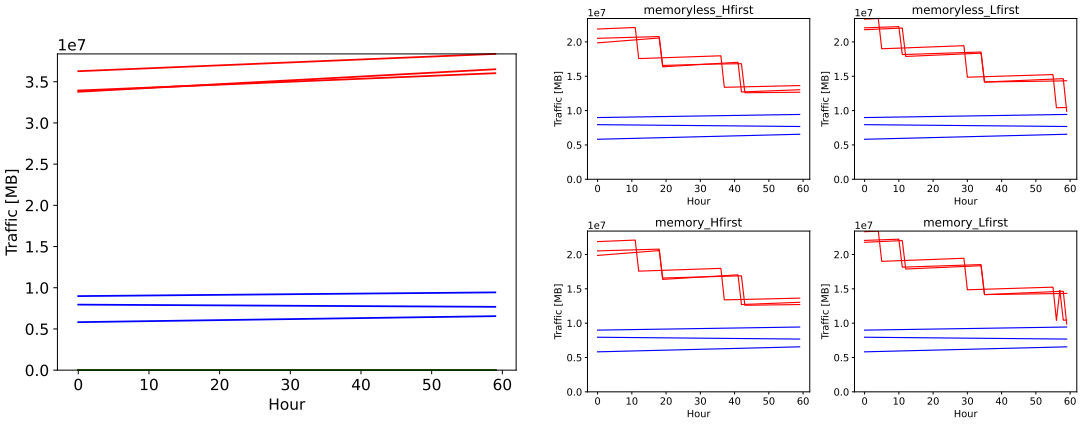

(a) Traffic injected in each MG **(b)** Traffic managed by each MG

Figure 3.14: Cluster analysis for Cardinality=8 and outages in July considering the traffic

Similar considerations can be made considering the traffic. Fig.3.14a shows, for each of the considered clusters, the incoming traffic. The clusters that perform

worse (whose traffic is traced in red) are also the ones subjected to higher traffic. Fig.3.14b shows the traffic managed by each MG using the same color choice used for the previous images. Since the traffic of incoming in a BS that is off is completely lost and cannot be redirected to another one, once the consumption exceeds the production and a BS is turned off, not only is there a drop in the energy consumed by the MG, but also in the traffic managed. The drop corresponds to the traffic incoming in the station that has been turned off.

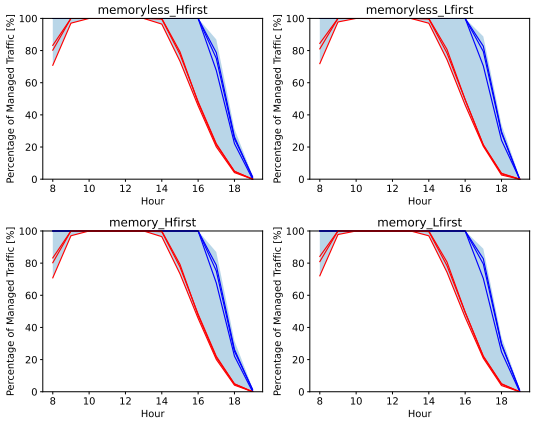

Figure 3.15: Percentage of traffic managed by the considered MGs during the day

In the previous section, Fig.3.7a shows the percentage of traffic managed by the MGs in the RAN. Fig.3.15 shows the same results but it highlights the percentage of traffic managed by the considered MGs. This shows that, regardless of the used approach (i.e. memory or memoryless, and giving priority to BSs with high or low traffic) the MGs that perform the best during the considered time slots tend to have high performance with respect to the others throughout the day. Vice versa, the daily performance of the MGs with the lowest percentage of managed traffic during the considered time slot is always low during the day.

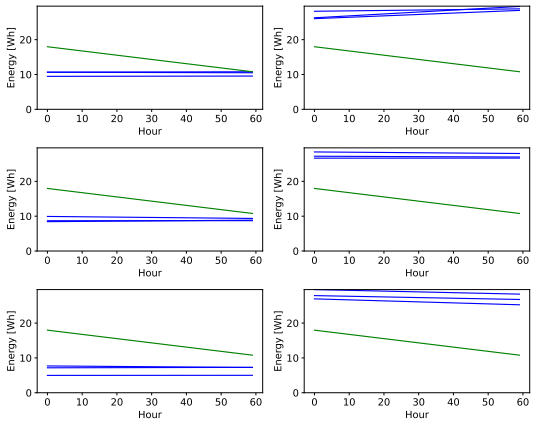

(a) Energy required by each BS with respect to the average production

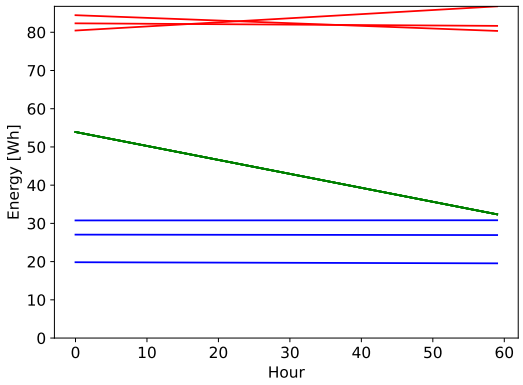

(b) Total consumption of the MGs

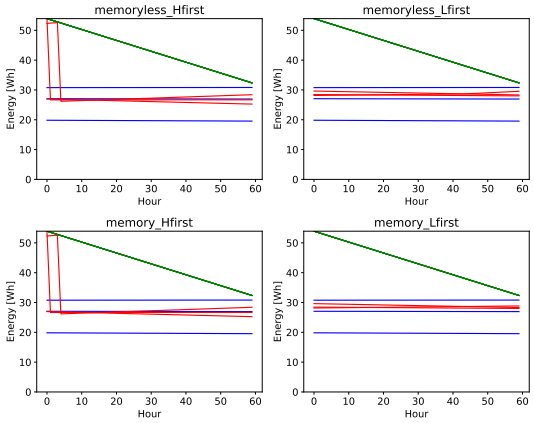

(c) Energy consumed by each observed MG

Figure 3.16: Cluster analysis for Cardinality=3 and outages in July

Figures 3.16, 3.17, and 3.18 show the same results obtained when the BSs are grouped in clusters with cardinality equal to 3. As in the case with cardinality equal to 8, Fig.3.16a and 3.16c shows that in the best-performing clusters, all the BSs consume less energy than the one produced by the PV panels, whereas the worst-performing ones contain BSs whose production alone is not enough to make the BS itself works. Fig.3.17a shows the traffic injected in each cluster. Again, it is evident that the worst-performing clusters are the ones with the higher traffic since the traffic is strictly correlated with the energy required by the BSs to work. Lastly, Fig.3.18 shows that the behavior of the clusters considering how good they perform with respect to the others in the RAN is fairly constant during the day.

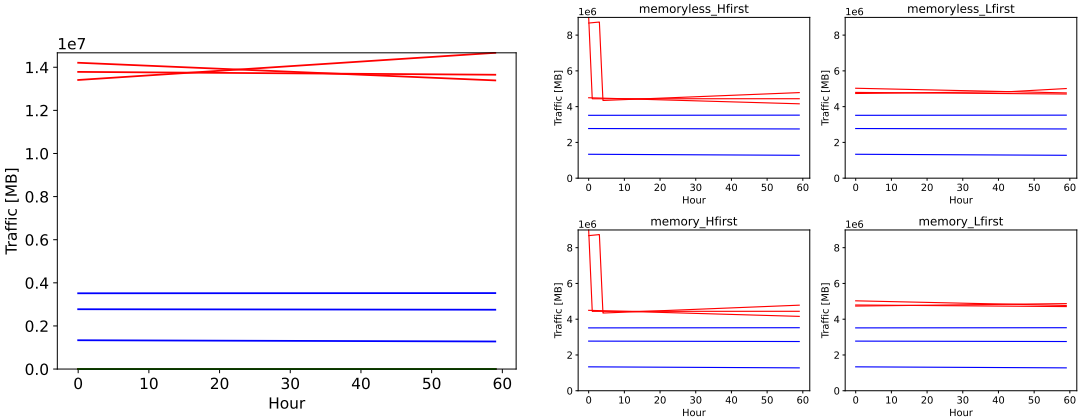

(a) Traffic injected in each MG **(b)** Traffic managed by each MG

Figure 3.17: Cluster analysis for Cardinality=8 and outages in July considering the traffic

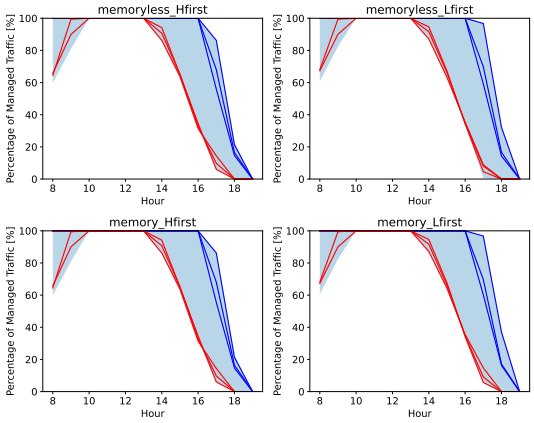

Figure 3.18: Percentage of traffic managed by the considered MGs during the day

3.4 Analyzing best-performing and worst-performing clusters changing clustering technique

In sec.3.3, the observed clusters were the best- and worst-performing ones in a scenario where the MGs were created with either cardinality 3 or 8, and by putting together BSs with similar characteristics with respect to incoming traffic, which means that the clusters were homogeneous. In this section, the goal is to understand how the clustering technique used affects the results by analyzing the best- and

worst-performing clusters in a heterogeneous scenario.

In order to create the new clusters, an ad hoc version of the k-means approach has been used. The algorithm is used to group together elements that have the highest distance from one another.

Starting again by analyzing the case of PGOs happening in July, and considering clusters with cardinality 8, the simulations were done using the four strategies proposed in sec.3.2 for energy management.

For the selection of the clusters, the same time slot considered for the homogeneous case has been considered.

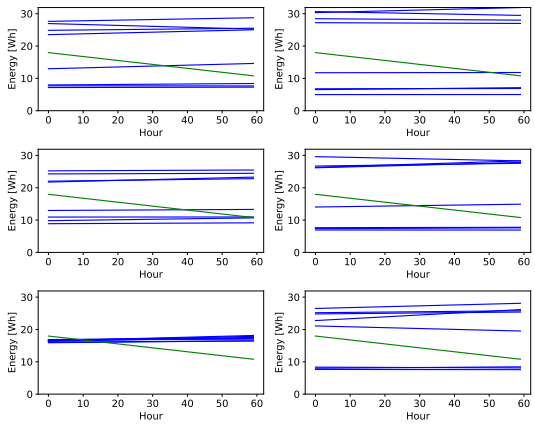

(a) Energy required by each BS with respect to the average production

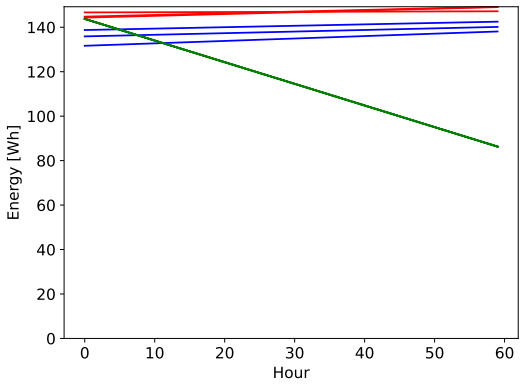

(b) Total consumption of the MGs

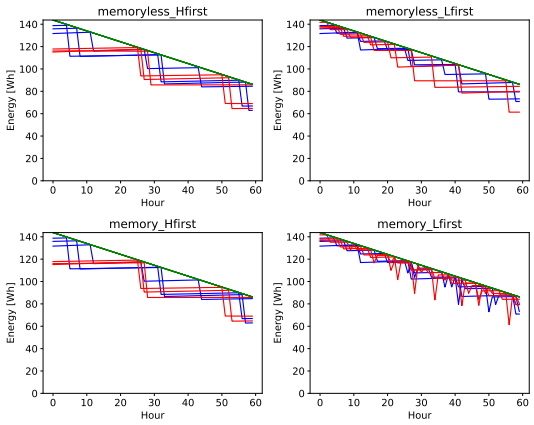

(c) Energy consumed by each observed MG

Figure 3.19: Cluster analysis for Cardinality=8 and outages in July using heterogeneous MGs

Fig.3.19a shows the energy required by each BS in each of the six considered

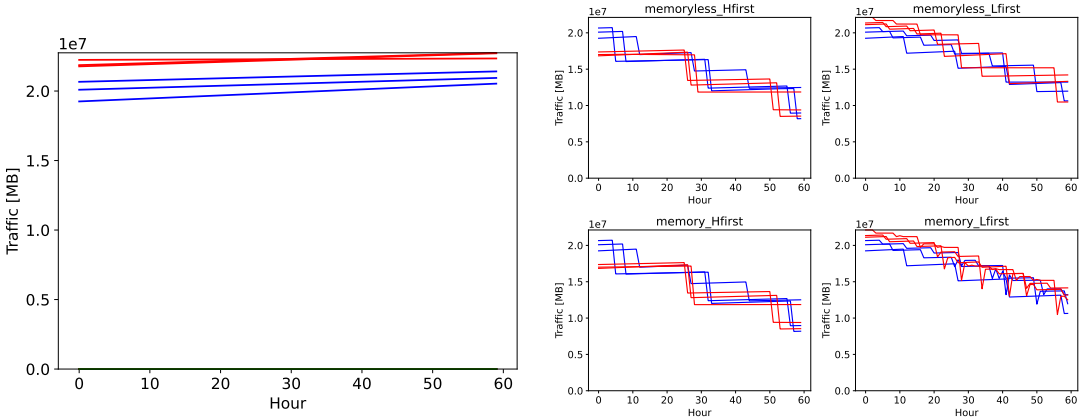

(a) Traffic injected in each MG **(b)** Traffic managed by each MG

Figure 3.20: Cluster analysis for Cardinality=8 and outages in July considering the traffic

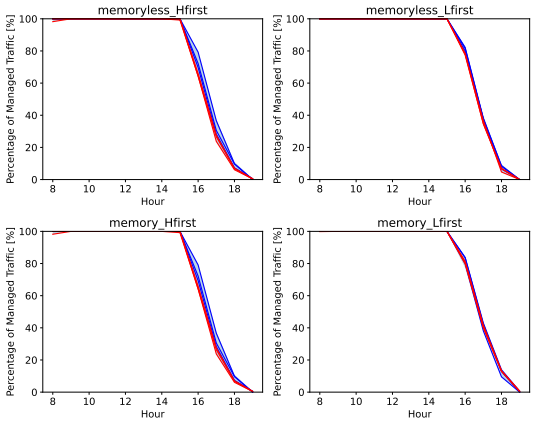

Figure 3.21: Percentage of traffic managed by the considered MGs during the day

clusters to work. As in the previous cases, the three best-performing MGs are on the left, and the three worst-performing on the right. Differently from the homogeneous case, each cluster presents both BSs whose production is enough to make the station work and BSs with a consumption higher than the production. The difference between the best- and worst-performing clusters can be seen in Fig.3.19c, where the total energy required by each cluster is reported with respect to the production of the clusters. The best-performing clusters (in blue) are the ones that require less energy to work, i.e. the ones that are subjected to a lower load as shown in Fig.3.20a and 3.20b, which report respectively the traffic injected in each BS of each of the six observed clusters and the total load for each of the

MGs. Comparing Fig.3.19b and Fig.3.13b in the previous section, it is possible to notice that in the previous case, the lines representing total energy required by the best-performing MGs were further from the ones of the worst-performing MGs with respect to the current case.

As in the previous section, the percentage of managed traffic of the MGs during the day with respect to the minimum and maximum values in the RAN has been reported in Fig.3.21. In this case, the range representing the variation of the performances in the RAN is much narrower with respect to the homogeneous case due to the fact that in a cluster there are both low-loaded BSs and high-loaded BSs, and the former can compensate for the latter since they do not need all the energy produced y their PV panels.

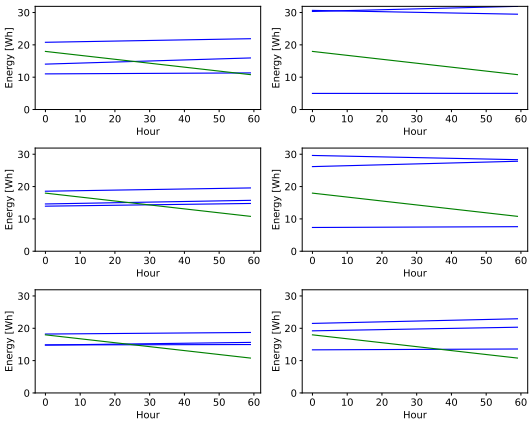

(a) Energy required by each BS with respect to the average production

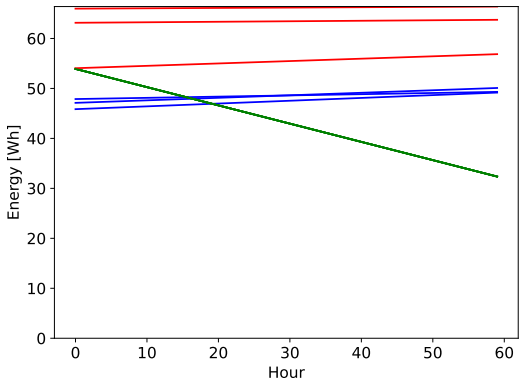

(b) Total consumption of the MGs

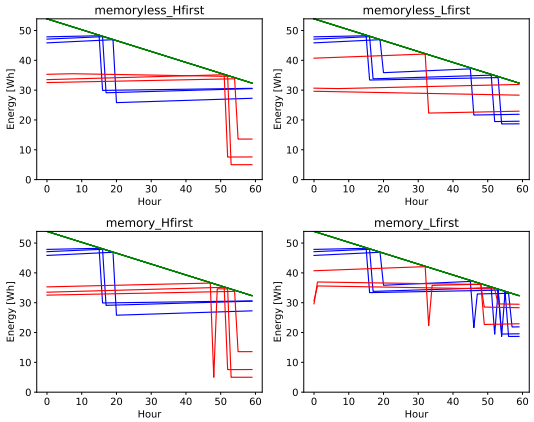

(c) Energy consumed by each observed MG

Figure 3.22: Cluster analysis for Cardinality=3 and outages in July using heterogeneous MGs

The same simulations have been done for the case in which the cardinality was set to 3, and the results are reported in Fig.3.22 and 3.20. Analyzing the energy required by each BS in Fig.3.22a, it is interesting to notice that even in the best-performing scenarios, all the BSs require more energy than the one they produce. In this case, it is evident how much impact does the MG have on the performance of the cluster as, without the possibility to exchange energy with one another, none of the BS would be able to work using just the energy from the PV panels. Considering the total energy required by each cluster, the difference between cluster that works well and those that does not is less evident with respect to the homogeneous case.

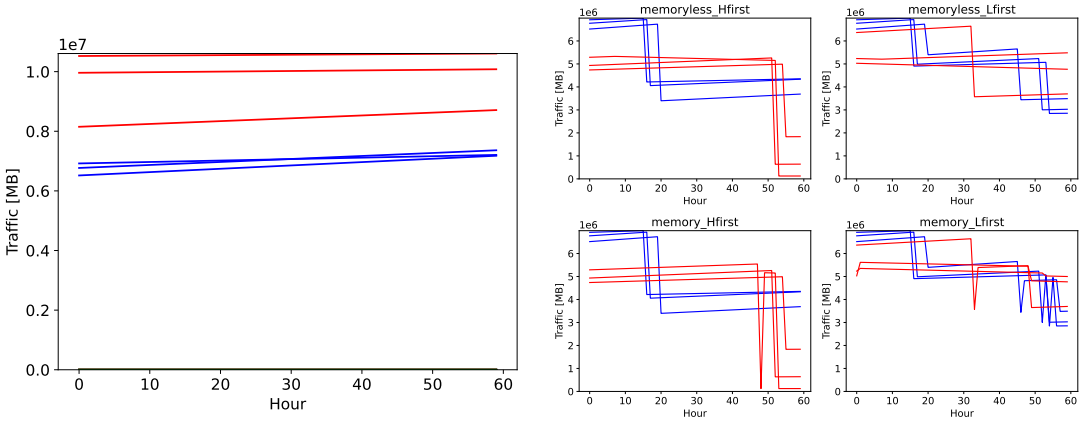

(a) Traffic injected in each MG **(b)** Traffic managed by each MG

Figure 3.23: Cluster analysis for Cardinality=3 and outages in July considering the traffic

Similarly to the case with cardinality equal to 8, if we consider the behavior of the MGs during a whole day, as shown in Fig.3.24, it is possible to notice that while clusters performing the best during the considered time slot are performing well throughout the day, those performing the worst during the same time slot vary their performances during the day. Also, the range of the considered performance parameter considering all the MGs in the RAN is wider than in the case with cardinality equal to 8, which shows again that larger clusters tend to have a behavior that is more similar to one another, whereas smaller ones have a behavior that depends more on the characteristics of the BSs in the MG.

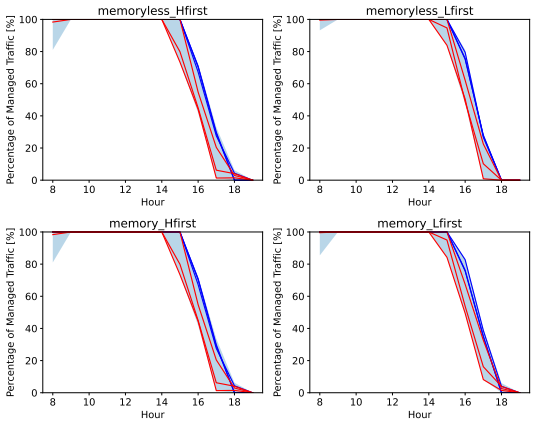

Figure 3.24: Percentage of traffic managed by the considered MGs during the day

3.5 Usage of batteries to avoid wastes

In all the cases analyzed in the previous parts, given a strategy for the management of energy, the performance only depends on the current energy produced by the BSs and by the energy they require, i.e. $P_i^{(t)}$ and $E_i^{(t)}$.

Considering the previous results, in many cases, the total consumption of an MG is lower than the production, $P^{(t)} > C^{(t)}$, but the delta between the two values is not enough to turn on another BS. The surplus of energy in these cases has always been wasted. A good solution to improve the performance of the whole system would be the addition of batteries to save the excess energy and to use it later.

In this section, three different scenarios will be compared:

- The standard scenario considered in the previous parts in which no battery is employed. It will be referred to in the images as *no_battery*.
- A scenario in which every MG has a battery collecting energy that can be used in every moment. It will be referred to in the images as *simple_battery*.
- A scenario in which every MG has a battery collecting energy, but the extraction of energy from the battery is inhibited according to a logic that will be explained later. It will be referred to in the images as *time_battery*.

The idea of using a single battery for each MG, and not one for every BS, is derived from the fact that, since in this scenario the losses in the energy transfer from one BS to another are not yet considered, having one battery for each Mg or one for each BS is equivalent.

As said before, in the third scenario, the energy from the battery is not always available. This is done considering the fact that it may require multiple time slots to accumulate the energy required by a non-active BS to work, and, as soon as this level of energy is reached, the BS is on for just one time slot. This behavior may lead to continuous churning. Instead, it is possible to inhibit the usage of the battery for a period of time to ensure that the BS that is turned on using the energy from the battery will remain on for a certain amount of time slots.

In order to evaluate the inhibition time of the battery, two problems have been formulated, the first in which the case when the number of active BSs decreases through time and the second in which it is increasing.

The first can be formulated as follows:

Problem
Consider an MG containing N BS. When the current energy consumed by the active BSs is higher than the energy produced, a BS is turned off, whereas, when the production is enough to turn on another BS, the BS is turned on. The overproduced energy is stored in a battery. The function $p(t)$ describes the energy produced by the MG through time and it is approximated as linear, $p(t) = C_1 + (t - t_0)k$. The functions $c_1(t)$ and $c_0(t)$ represent respectively the consumption of the MG when $b + 1$ and b BSs are active, and they are again approximated as linear, $c_1(t) = C_1 + (t - t_0)n$ and $c_0(t) = C_0 + (t - t_0)k$. At t_0 the consumption of $b + 1$ BSs saturates the production resulting in the turning off of a BS. Calling t_2 the time at which the consumption of b BSs saturates the consumption, find t_1, which is the moment in which the energy in the battery is enough to turn on another BS until t_2.

Since the problem reflects a real case scenario, it is logical to assume $0 < C_0 < C_1$. In fact, when a BS is turned off, the consumption should decrease, and the total consumption of any number of BSs should always be non-negative. Since the problem considers the case in which the number of active BS is decreasing, it is possible to assume $k < m$ and $k < n$, otherwise the consumption would not saturate the production.

In order to better understand the problem, Fig.3.25 reports the plot of the problem variables.

Since we are interested in the inhibition time, which is $t_1 - t_0$ we can apply the transformation $t \to t - t_0$. Moreover, to simplify the computation, we can apply a similar transformation to the ordinate axis translating the reference system by a quantity equal to C_1. Applying these transformations, the equations become $p(t) = C + tk$, $c_0(t) = tk$, and $c_1(t) = C + tn$, where $C = C_1 - C_0$. The solution of the problem is $x = t_1 - t_0$, whereas a new variable is defined as $T = t_2 - t_0$, representing t_2 in the new reference system.

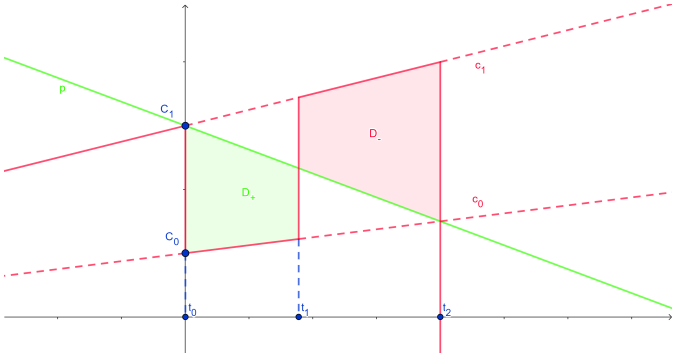

Figure 3.25: Plot of production and consumption when the number of active BSs is decreasing

The energy saved in the battery corresponds to the difference between the consumption of the MG and the total energy produced, so the total energy saved in the battery between t_0 and t_1 is equal to:

$$D_+ = \int_0^x [p(t) - c_0(t)]\,dx = \int_0^x [kt + C - mt]\,dx = C*t + \frac{k-m}{2}t^2\Big|_0^x = Cx + \frac{k-m}{2}x^2 \tag{3.5}$$

The energy required for another BS to be activated corresponds to the difference between the energy required by b BSs and the total energy produced. This corresponds to :

$$D_- = \int_x^T [c_1(t) - p(t)]\,dx = \int_x^T [nt + C - kt - C]\,dx = \frac{n-k}{2}t^2\Big|_x^T = \frac{n-k}{2}x^2 \tag{3.6}$$

The solution to the problem can be easily obtained by solving the following equation:

$$D_+ = D_- \tag{3.7}$$

It is also possible to notice that the values T and C are correlated since C is the difference between $p(0)$ and $C_0(0)$ and T is the abscissa of the intersection of $p(t)$ and $c_0(t)$. From this fact, it is possible to write the following relation between T and C:

$$C = T(m - k) \tag{3.8}$$

Substituting 3.5 and 3.6 in 3.7, we obtain:

$$(n-k)T^2 - (n-k)x^2 = (k-m)x^2 + 2Cx \tag{3.9}$$

Solving the equation substituting 3.8, the inhibition time is obtained:

$$x = \begin{cases} T\frac{m-k}{n-m}(-1+\sqrt{1-\frac{(k-n)(n-m)}{(m-k)^2}}) & \text{if } m \neq n, \\ \frac{T}{2} & \text{if } m = n \end{cases} \tag{3.10}$$

Similarly, it is possible to formulate another problem when the number of active BSs is increasing:

Problem
Consider an MG containing N BS. When the current energy consumed by the active BSs is higher than the energy produced, a BS is turned off, whereas, when the production is enough to turn on another BS, the BS is turned on. The overproduced energy is stored in a battery. The function $p(t)$ describes the energy produced by the MG through time and it is approximated as linear, $p(t) = C_0 + (t - t_0)k$. The functions $c_1(t)$ and $c_0(t)$ represent respectively the consumption of the MG when $b + 1$ and b BSs are active, and they are again approximated as linear, $c_1(t) = C_1 + (t - t_0)n$ and $c_0(t) = C_0 + (t - t_0)k$. At t_0 the number of active BSs passes from $b - 1$ to b. Calling t_2 the time at which the number of active BSs would increase again if the system were not to use the battery, find t_1, which is the moment in which the energy in the battery is enough to turn on another BS until t_2.

For analogous reasons as in the previous problem, it is possible to assume $C_1 > C_0 > 0$, $K > n$, and $k > m$. Moreover, the same transformations are used to obtain the following: $p(t) = tk$, $c_0(t) = tk$, and $c_1(t) = C + tn$, where $C = C_1 - C_0$. Again, the geometry of the problem is proposed in Fig.3.26.

Again, the energy saved in the battery can be expressed as the integral of the difference between the energy produced by all the PV panels in the MG and the energy consumed by b BSs:

$$D_+ = \int_0^x [p(t) - c_0(t)]\,dx = \int_0^x [kt + C - mt]\,dx = Ct + \frac{k-m}{2}t^2\Big|_0^x = Cx + \frac{k-m}{2}x^2 \tag{3.11}$$

Whereas, the energy required to turn on the $b + 1$-th BS is the integral of the difference between the energy consumed by $b + 1$ BSs and the energy produced by the MG:

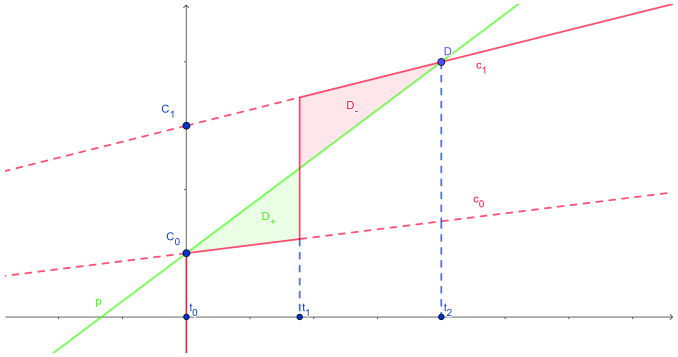

Figure 3.26: Plot of production and consumption when the number of active BSs is increasing

$$D_- = \int_x^T [c_1(t) - p(t)]\,dx = Ct + \frac{n-k}{2}t^2 + Ct\Big|_x^T = CT + \frac{n-k}{T}x^2 - Cx - \frac{n-k}{2}x^2 \tag{3.12}$$

As in the previous case, it is possible to write a relationship between C and T, which is:

$$C = T(k-n) \tag{3.13}$$

The solution of the problem can be again found by solving 3.7. Substituting 3.12 and 3.12 in 3.7, one obtains:

$$\frac{n-k}{2}T^2 + Ct + \frac{k-n}{2}x^2 - Cx = \frac{k-m}{2}x^2 \tag{3.14}$$

The solution of the equation, using 3.13, is:

$$x = \begin{cases} T\frac{k-n}{m-n}(1 + \sqrt{1 - \frac{m-n}{k-n}}) & \text{if } m \neq n, \\ \frac{T}{2} & \text{if } m = n \end{cases} \tag{3.15}$$

To compare the performance of these three approaches, the simulations were done considering only homogeneous clusters with cardinality equal to 8. Moreover, the PGOs used for the simulations were synthetic ones, in the month of July, considering a time range from 8 A.M. to 8 P.M. As in sec.3.3, only the three best-performing and the three worst-performing clusters were considered.

In order to better understand the behavior of the clusters using the different approaches, graphs were made considering the three worst-performing clusters during the PGOs at 8 A.M. and 4 P.M. The choice of selecting only the worst-performing clusters for the graphs is dictated by the fact that, as seen in sec. 3.3, in

most cases, the best-performing cluster can achieve maximum performance without any additional aid. The choice of the time slots is done to consider a case in which the number of active BSs is increasing and one in which it is decreasing.

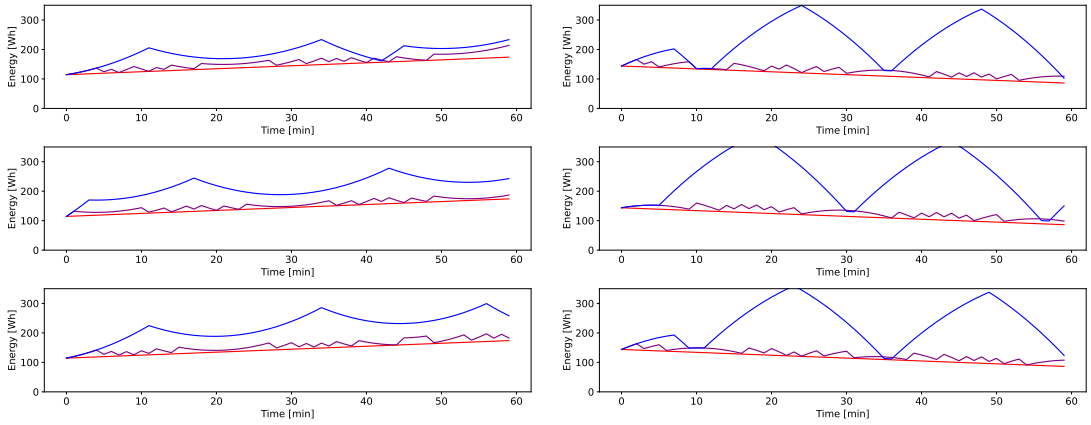

(a) 8 A.M. **(b)** 4 P.M.

Figure 3.27: Amount of available energy in each cluster in the three different scenarios: *no_battery* (red), *simple_battery* (purple), and *time_battery* (blue)

Fig.3.27 reports for each cluster the available energy in each time slot. In the *no_battery* case, it corresponds to the energy coming from the PV panels, whereas, in the other cases, it is the sum of the energy produced by the PV panels and the one stored in the batteries. It is possible to notice that, since the PV panels produce the same in each scenario, the *no_battery* case is always the one with less energy. In the *time_battery* case, the energy tends to reach higher values as the cluster is accumulating energy without using it as soon as it is possible. The spikes in the graphs in the *simple_battery* case and in the *time_battery* case represent the charge and discharge of the batteries.

Fig.3.28 shows the energy consumed by each cluster. In the *simple_battery* and *time_battery* cases, the consumption can be higher thanks to the usage of batteries. This corresponds to another BS turning on. The difference is that in the latter case, the consumption increases after the inhibition time when the energy from the battery is available. The inhibition time of the batteries is reported in Fig.3.29, where the value reported for each time instant represents the amount of time that is still to pass before the energy from the battery is available. When the time becomes negative, the battery is being used and the value represents for how long.

Lastly, Fig.3.30 shows the percentage of traffic managed by each cluster in each time slot. It is possible to notice that, the cases in which batteries are implemented, always perform better.

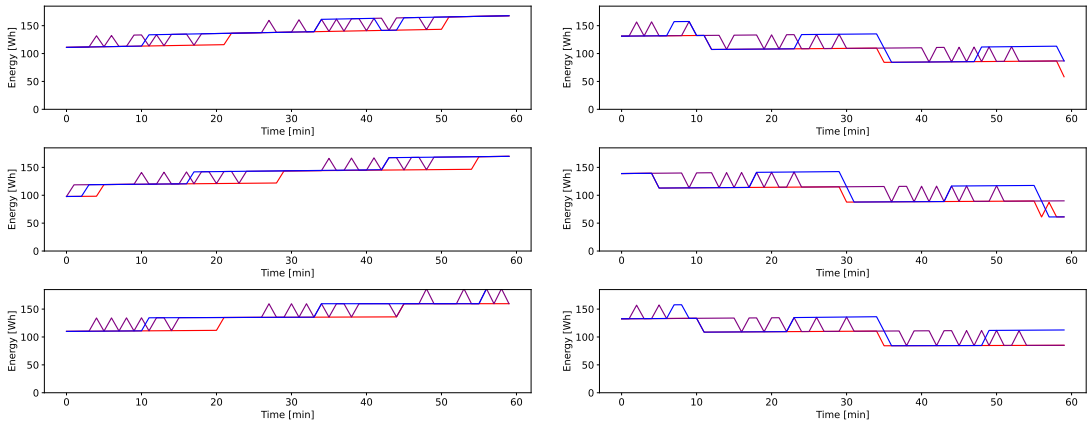

(a) 8 A.M. **(b)** 4 P.M.

Figure 3.28: Amount of energy consumed by each cluster in the three different scenarios: *no_battery* (red), *simple_battery* (purple), and *time_battery* (blue)

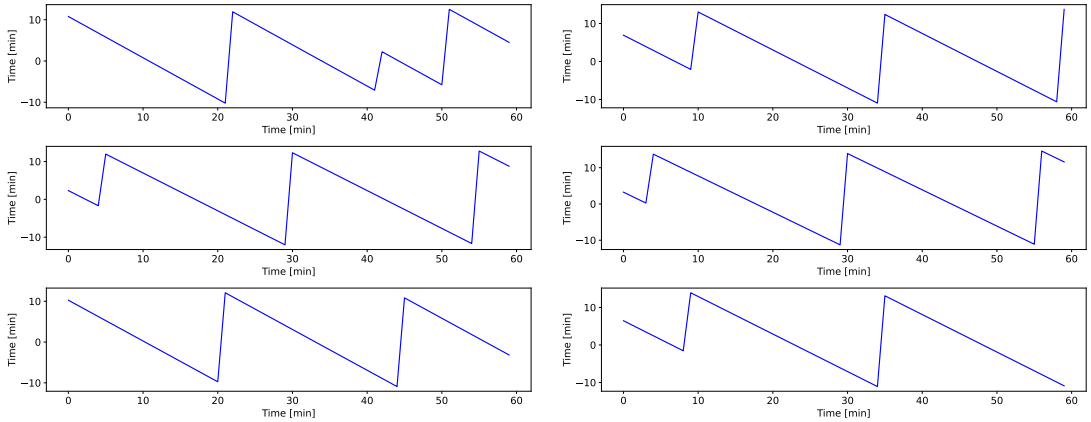

(a) 8 A.M. **(b)** 4 P.M.

Figure 3.29: Inhibition time for each cluster in the *time_battery* scenario

Table 3.1 reports the percentage of traffic managed by each cluster during the PGOs in the considered time period in each of the three scenarios. Moreover, the percentage of traffic managed by the clusters together has been computed. Observing the results, it is evident that implementing batteries increases the performance of the system. Adding the inhibition time leads to a slight decrease in the performance, but, as seen in Fig.3.28, it diminishes the churning of the stations.

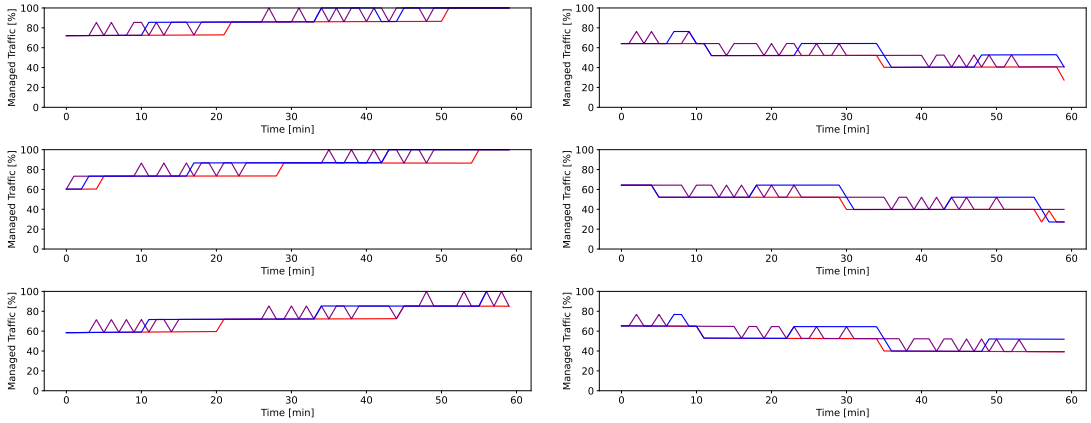

(a) 8 A.M. **(b)** 4 P.M.

Figure 3.30: percentage of traffic managed by each cluster in the three different scenarios: *no_battery* (red), *simple_battery* (purple), and *time_battery* (blue)

Case	Cluster 1	Cluster 2	Cluster 3	Cluster 4	Cluster 5	Cluster 6	Total
no_battery	80.38	80.56	84.77	66.34	64.08	66.04	68.38
simple_battery	81.95	82.62	86.23	69.14	67.18	69.07	71.13
time_battery	81.93	82.54	86.17	68.47	66.52	68.46	70.59

Table 3.1: Percentage of managed traffic

3.6 Adding losses in the exchange of energy and varying the production of energy

In the previous sections, the simulated environment was balanced, i.e. every BS in each cluster produced the same amount of energy, and ideal as no losses were present in the exchange of energy among BSs.

We now want to change this by varying the amount of energy produced in each BS by the PV panels, and by considering that transmitting energy on cables between the BSs produces a loss.

Given a BS, P_{max} is the energy produced in the previous cases and P_{new} is the one produced in the new scenario. The parameter ρ is defined as the ratio between P_{new} and P_{max}, i.e. $\rho = P_{new}/Pmax$.

In order to be fair between different clusters, each MG will be defined in the same way, which means that in all the clusters the i-th BS will produce the same. The number of parameters to be defined to represent the new production with respect to the previous is equal to the cardinality. The parameters are ρ_i, with $i = 1...C$, where C is the cardinality.

To consider losses, a matrix L was created, where $L_{i,j}$ represents the factor by which the energy sent by BS i to BS j must be multiplied in order to take in account the losses. All the elements in L are non-negative and smaller or equal to 1. The elements in the diagonal are equal to 1 as there is no loss when the energy remains in the same BS.

For this part, three approaches to the energy management were compared:

- *LFirst*: it is the same approach explained in sec.3.2 referred to as *memoryless_LFirst*.
- *HFirst*: it is the same approach explained in sec.3.2 referred to as *memoryless_HFirst*.
- *Optimal*: the optimal approach is obtained by using Gurobi, a mathematical optimization problem, to find the best allocation of energy. This technique for the management of energy is added as a reference point since the implementation in a real-case scenario is not easy due to the fact that the computation requires more time.

For the *Optimal* approach, the problem to be solved was the following:

Problem

Consider an MG containing N BS. Each BS i in a certain time instant t produces through a set of PV panels an amount of energy equal to P_i^t, the traffic load incoming is T_i^t, and the energy required by the BS i to remain on is E_i^t. If a BS receives (from both the PV panels and other stations) at least C_i^t, it will remain active and manage all the incoming traffic, else it will turn off and manage none. The state of a BS i at time t is expressed by a variable $S_i^{(t)}$ which is equal to 1 if the BS is active and 0 if it is off. Knowing that the BSs can exchange energy, but while doing this they incur losses such that if a quantity $E_{i,j}^{(t)}$ of energy is sent from BS i to BS j, only $E_{i,j}^{(t)} * L_{i,j}$ arrives at the destination (with $0 \leq L_{i,j} \leq 1$), find the best allocation of energy to maximize the traffic managed.

$$
\begin{aligned}
\max \quad & \sum_{i=1}^{N} T_i^t S_i^t & \\
\text{subject to} \quad & C_i^t \cdot S_i^t \leq P_i^t - \sum_{i=1}^{N} E_{i,j}^t + \sum_{j=1}^{N} E_{j,i}^t & \forall i \\
& E_{i,j}^t \geq 0 & \forall i, j \\
& E_{i,j}^t \leq P_i^t + \sum_{j=1}^{N} E_{j,i}^t & \forall i, j
\end{aligned}
$$

At first, the values ρ_i were randomly chosen. Then, in order to understand if there is an optimal placement for the PV panels, all the production was placed in a single BS and it was evaluated with which BS the best performance was reached.

Considering ρ the vector containing all the ρ_i, i.e. $\rho = \rho_i, i = 1...N$, the vector in the random case was $\rho =$. In order to be fair among the clusters, the BSs in each MG were ordered in decreasing order with respect to the average traffic during the day. Since the sum of all the ρ_i in the random case is equal to 5, in the case in which the production is on the i-th BS ρ_i will be equal to 5 and any other ρ_j will be 0. Table 3.2 reports all the values of the ρ_i in each of the considered cases.

Active BSs	ρ_1	ρ_2	ρ_3	ρ_4	ρ_5	ρ_6	ρ_7	ρ_8
1	5	0	0	0	0	0	0	0
2	0	5	0	0	0	0	0	0
3	0	0	5	0	0	0	0	0
4	0	0	0	5	0	0	0	0
5	0	0	0	0	5	0	0	0
6	0	0	0	0	0	5	0	0
7	0	0	0	0	0	0	5	0
8	0	0	0	0	0	0	0	5
random	0.8	1.0	0.4	0.9	0	0.9	1.0	0

Table 3.2: Values of ρ in the considered cases

As in the previous sections, the simulation considers only the three best-performing and the three worst-performing clusters and uses synthetic traces for the PGOs happening between 8 A.M. and 8 P.M. in July.

Considering MGs with cardinality equal to 8, Fig.3.31 shows the results obtained, i.e. the percentage of managed traffic using each of the previously explained methods.

Table 3.3 reports the percentage of managed traffic during the complete time period for each case. Comparing the techniques, the *Optimal* is always the best, as expected. Among the other two, the $LFirst$ typically gives better results, so it is possible to deduce that it is better to give priority to BS with a higher load even when losses are present. Regarding the placement of the energy source, it is clear that dividing the production always gives better results.

At this point, considering one of the best configurations, which is when the production is placed in the 8-th BS[1], the cases in which the production is equally

[1]This configuration is always among the best-performing for each scenario, and, in the *Optimal*

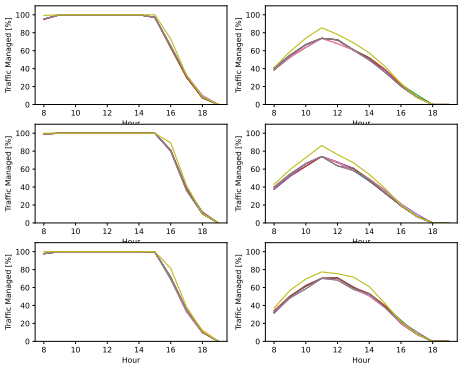

(a) HFirst

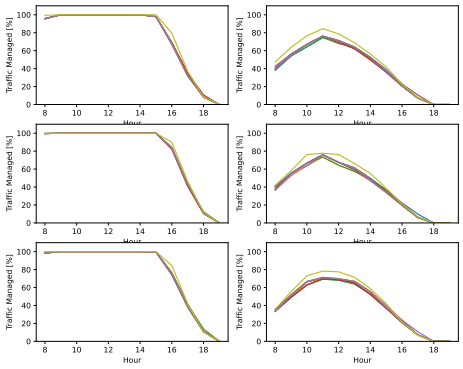

(b) LFirst

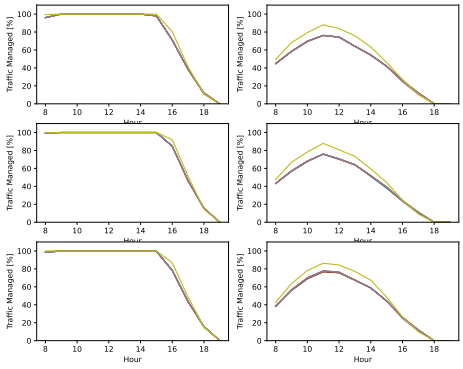

(c) Optimal

Figure 3.31: Percentage of traffic managed by each cluster

divided between two BSs, one of which is always the 8-th, have been considered. The new configurations are reported in Table 3.4. The results obtained with this configuration have been used as a baseline. This procedure has been done to find out if dividing the production between the BSs always improve the performance, and if there is an optimal allocation for the PV panels.

Fig.3.32 reports the results. The values plotted are not the percentage of traffic managed but difference of the percentage of managed traffic between the considered case and the baseline. Except for some cases, dividing the PV panels between more BSs leads to an increase in the performance.

scenario, it is the best performing

Active BSs	LFirst	HFirst	Optimal
1	44.27	43.74	46.90
2	43.84	43.96	47.06
3	43.86	43.95	47.04
4	44.08	43.81	47.04
5	44.58	43.87	47.07
6	44.78	43.55	47.04
7	44.61	43.36	47.05
8	44.50	43.56	47.13
random	47.82	47.61	51.51

Table 3.3: Percentage of managed traffic in the considered cases

Active BSs	ρ_1	ρ_2	ρ_3	ρ_4	ρ_5	ρ_6	ρ_7	ρ_8
1-8	2.5	0	0	0	0	0	0	2.5
2-8	0	2.5	0	0	0	0	0	2.5
3-8	0	0	2.5	0	0	0	0	2.5
4-8	0	0	0	2.5	0	0	0	2.5
5-8	0	0	0	0	2.5	0	0	2.5
6-8	0	0	0	0	0	2.5	0	2.5
7-8	0	0	0	0	0	0	2.5	2.5

Table 3.4: Values of ρ in the considered cases

A procedure similar to the one explained until now has been applied to the case in which the cardinality of the MGs is equal to 3. This time, since the number of possible combinations of active BS is small, all the possibility were taken into account. The possible configurations are reported in Table.3.5 with the relative value of ρ_i. All the values are chosen so that the sum of all the ρ_i in an MG is equal to 1.4.

Fig.3.33 shows the percentage of traffic managed by each cluster. Since there are fewer degrees of freedom when the cardinality is lower, as expected, all the configurations tend to have a very similar behavior. In the cases in which one or more configurations perform slightly better, those configurations are always the ones in which the production is distributed either on two or three BSs.

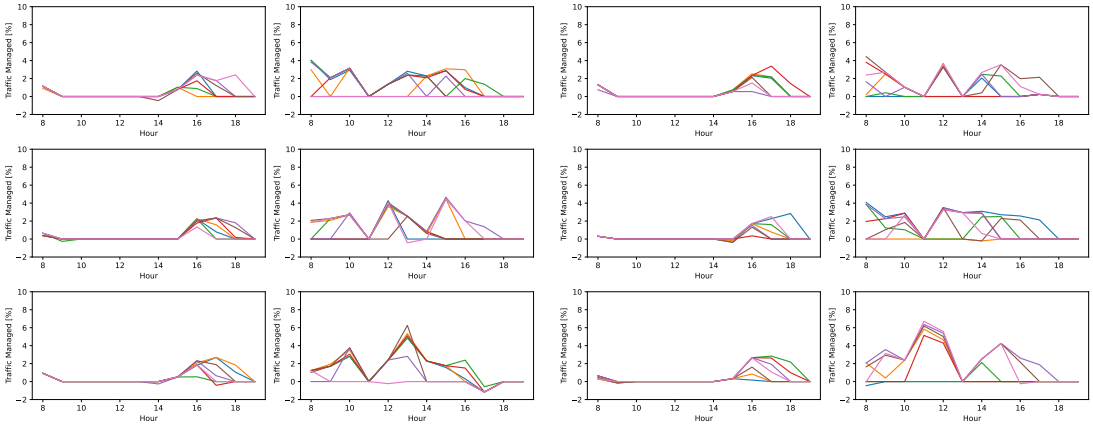

(a) HFirst **(b)** LFirst

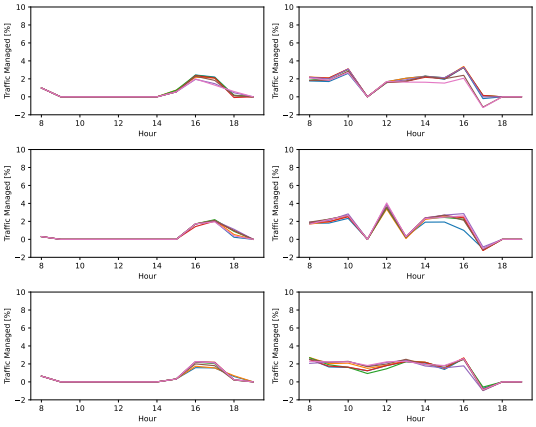

(c) Optimal

Figure 3.32: Difference of percentage of traffic managed by each cluster with respect to the baseline

Active BSs	ρ_1	ρ_2	ρ_3
1	1.4	0	0
2	0	1.4	0
3	0	0	1.4
1-2	0.7	0.7	0
1-3	0.7	0	0.7
2-3	0	0.7	0.7
1-2-3	0.47	0.47	0.47

Table 3.5: Values of ρ in the considered cases

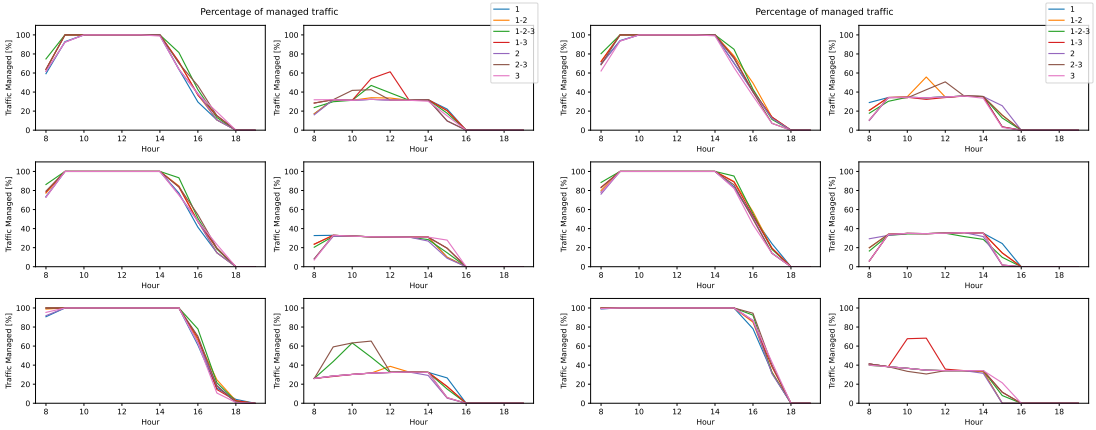

(a) HFirst

(b) LFirst

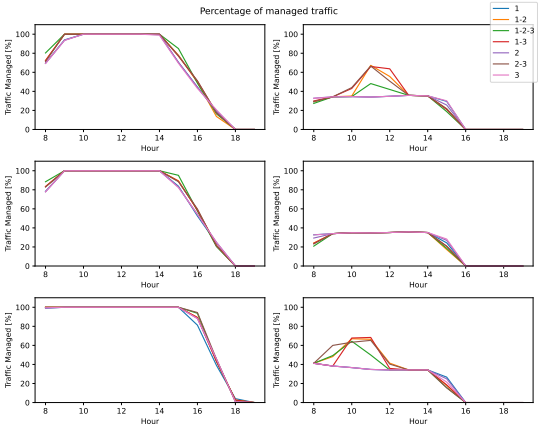

(c) Optimal

Figure 3.33: Percentage of traffic managed by each cluster

3.7 Taking into account the topology of the MGs

Up until now, the topology of the MGs was never taken into account. This is due to the fact that it only makes sense to consider the topology when losses are present. In fact, if there are no losses, as long as the graph representing the MG is connected, there is always a path between two nodes, and no energy is lost.

Now that losses are present, it is interesting to take into account the problem of the best placement of the PV panels as done in the previous section, with respect to the topology of the network.

In order to do this, the same procedure explained in the previous section for the MGs with cardinality equal to 8 has been applied. To do this, a linear topology has been considered for each MG. The BSs in the MG are set in decreasing order of average traffic during the day.

The linear topology presents two main advantages for this study. First, it is a topology that allows to use of the minimum number of links to create a connected graph, and second, it is the topology with the maximum diameter, allowing to stress the system, and analyzing the performance in the worst-case scenario.

Since the focus of this part is analyzing how the topology affects the performance, and not the energy management algorithm, only the optimal results were computed.

Given the topology of the network, and considering a loss of 20% on each link, the terms $L_{i,j}$ are equal to $0.8^{|i-j|}$.

Proceeding by simulating the presence of PV panels in just one BS, results shown in Table 3.6 and Fig.3.34 were found.

Active BSs	Percentage of managed traffic
1	39.78
2	41.24
3	38.81
4	41.11
5	40.39
6	42.08
7	40.56
8	40.94

Table 3.6: Percentage of managed traffic

It can be clearly seen that the case in which the production is on the 6th BS is the best one. It makes sense considering the fact that this BS has a central position on the bus. This case has been considered as a baseline for the next step.

Dividing the production on two BSs, one of which is the best of the single BS case, the results shown in Fig.3.35 were found. Again, each case shows improvement

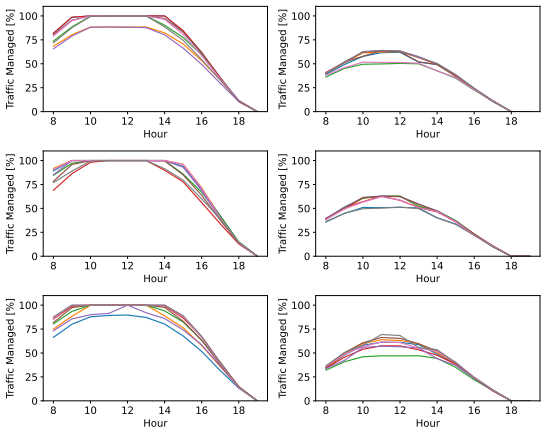

Figure 3.34: Percentage of traffic managed by each cluster considering a BUS topology and production in a single BS

with respect to the single-BS one, and, in most of the cases, the configuration with the 4th and 6th BS active is the one that reaches the best performance.

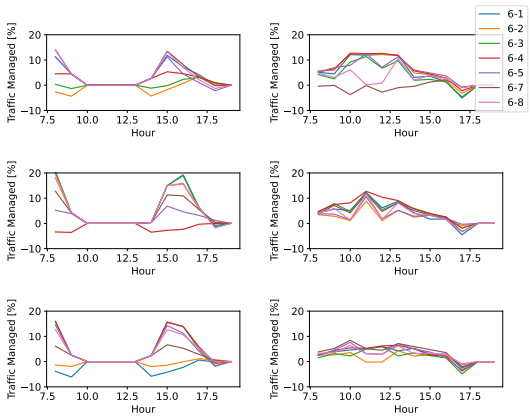

Figure 3.35: Difference of traffic managed by each cluster considering a BUS topology and production in two BS and the baseline

Considering the cluster in the low left corner, it is possible to notice that at 8 A.M. the various configurations have different performances, with configuration 6-1 having a performance lower than when the energy is produced in just BS 6. The same configuration has poor performances from 2 P.M. to 5 P.M. Configuration 6-2 is also performing poorly in the same time period, achieving no improvement with respect to the single-producing BS case. To understand what influences this behavior, the energy consumed by each BS in each configuration has been plotted

in Fig.3.36a and the number of active BSs has been reported in Fig.3.36b.

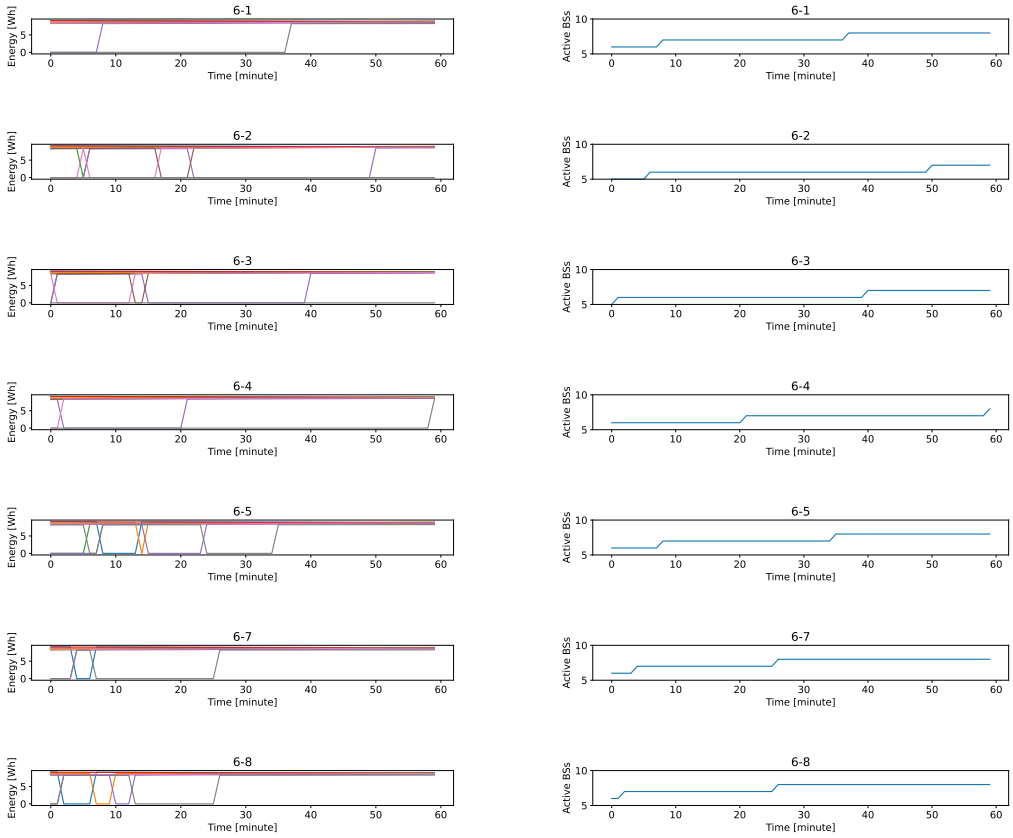

(a) Energy consumed by BSs in each configuration at 8 A.M.

(b) Number of active BSs in each configuration at 8 A.M.

Figure 3.36: Cluster analysis considering each configuration at 8 A.M.

The two previously mentioned configurations are among the ones with the lowest number of active BSs.

Chapter 4

Conclusions

In Sec.3, the main characteristics of the considered system have been analyzed, studying the performance of the system itself under different working conditions. In this section, the goal is to summarize the results obtained before, deducing which is the best configuration for the system to maximize the performance. In the case study, the performance was evaluated based on the percentage of traffic managed by the system.

Starting by considering the strategies used to manage the energy produced by the MGs, as seen in Sec.3.2, different strategies give very similar results, but generally maintaining active BSs with higher traffic is better than activating BSs with lower traffic, even if this allows for a higher number of BSs to stay active at the same time. The difference in the performance between the two cases considering the percentage of managed traffic during the most critical hours (i.e. when the production is not enough for the whole system to remain active) is usually between 1% and 4%. The implementation of memory in the strategies with the purpose of avoiding churning of the BSs is not a great solution, as seen by studying the rate at which the BSs switch state. Considering the percentage of managed traffic, the difference between the results with and without memory is very low, having just a peak at 3.6% in the morning hours (i.e. when production is low), but being usually less than 0.5%. As seen in Sec.3.6, the strategies studied in that section show results that are very similar to the ones obtained using the optimal strategies, meaning that additional work done trying to improve the used strategies would not give an improvement on the performance.

Considering how the type of MG, i.e. either homogeneous or heterogeneous, both typologies give similar results considering the average over all the MGs, but in the latter case all the MGs tend to have similar results with one another, whereas, in the former, the difference between the results obtained by the best-performing BSs and the ones obtained by the worst-performing ones is higher, as shown in Sec.3.3 and 3.4. The difference between performance of the best- and worst-performing

BSs considering the percentage of managed traffic in July with Cardinality 8 is lower than 16% in the heterogeneous case, whereas in the homogeneous it can reach up to 68%. It is important to note that the choice of the BSs to be placed in the same MG is not always a completely unbounded choice as the physical position of the BSs must be taken into account. In fact, aspects such as the distance between the BSs and the impossibility of connecting two BSs due to physical obstruction may interfere with the choices to be made. The distance between the BSs is also important as it impacts the losses in the transmission.

The usage of batteries, studied in Sec.3.5, shows a slight improvement in the performance of the system, allowing for 3% more of the incoming traffic to be managed. The strategy used to manage the energy stored in the battery does not impact the performance of the system, the difference in performance being less than 1%. However, the strategy may impact the switch rate of the BSs in the MGs as, as seen in the *simple_battery* strategy, some BSs tend to turn on for a small amount of time, sometimes even for just a single time-slot, and then turn off again, whereas in the *time_battery* strategy, the status of the BSs tends to remain the same for longer periods.

By differentiating the energy produced in each BS and considering losses, the performance gets worse, as shown in 3.6. The positioning of energy production does not seem to have an impact on the performance of the system, giving changes in the percentage of managed traffic which are smaller than 6% and, in most of the cases, lower than 3%. What really impacts in this case is the reduction of the total energy produced in the MG.

Considering instead the topology of the MGs, it is important to notice that this variable only impacts the system if sensible losses are present. If losses are negligible, the system can be considered a fully connected MG. As shown in 3.7, the placement of the energy production in an MG with a bus topology and with losses is more impactful than in a fully connected MG, reaching even 20% in the difference of percentage of managed traffic but there is not a perfect placement that optimizes the value for all the MGs.

In conclusion, the creation of Microgrids connecting radio Base Stations is a promising solution to make the telecom more resilient. The usage of Renewable Energy Sources allows to supply the system when the Power Grid is not supplying any energy due to an outage occurring.

Bibliography

[1] *Ericsson Mobility Report*. Tech. rep. November 2021. Ericsson, Nov. 2021 (cit. on p. 1).

[2] European Union Agency for Network and Information Security. *ENISA - Annual report telecom security incidents 2021*. Tech. rep. Tech. Rep July, 2021. July 2021 (cit. on pp. 1–3).

[3] European Union Agency for Network and Information Security. Tech. rep. URL: https://ciras.enisa.europa.eu/ (cit. on p. 1).

[4] H. Jones. «Going beyond reliability to robustness and resilience in space life support systems». In: *50th International Conference on Environmental Systems*. 2021 (cit. on p. 3).

[5] A. Cabrera-Tobar, F. Grimaccia, and S. Leva. «Energy Resilience in Telecommunication Networks: A Comprehensive Review of Strategies and Challenges». In: *Energies* 16 (2023), p. 6633 (cit. on pp. 3, 4).

[6] Hannah Ritchie. *What are the safest and cleanest sources of energy?* Published online at OurWorldInData.org. [Online Resource]. 2020. URL: https://ourworldindata.org/safest-sources-of-energy (cit. on p. 4).

[7] Yongrong Zhou, Yan Zhao, and Zhaoxing Ma. «Resilience analysis and improvement strategy of microgrid system considering new energy connection». In: *PloS One* 19 (2024), e0301910. DOI: 10.1371/journal.pone.0301910 (cit. on p. 4).

[8] M. Jafari, Z. Malekjamshidi, and J. Zhu. «Copper Loss Analysis of a Multi-winding High-Frequency Transformer for a Magnetically-Coupled Residential Microgrid». In: *IEEE Transactions on Industry Applications* 55.1 (Jan. 2019), pp. 283–297. DOI: 10.1109/TIA.2018.2864170 (cit. on p. 4).

[9] Chris Marnay, Spyros Chatzivasileiadis, Chad Abbey, Reza Iravani, Geza Joos, Pio Lombardi, Pierluigi Mancarella, and Jan von Appen. «Microgrid Evolution Roadmap». In: *2015 International Symposium on Smart Electric Distribution Systems and Technologies (EDST)*. 2015, pp. 139–144. DOI: 10.1109/SEDST.2015.7315197 (cit. on pp. 7, 8).

[10] Kumail Twaisan and Necaattin Barışçı. «Integrated Distributed Energy Resources (DER) and Microgrids: Modeling and Optimization of DERs». In: *Electronics* 11 (Sept. 2022), p. 2816. DOI: 10.3390/electronics11182816 (cit. on p. 8).

[11] Chijioke Agupugo, Husseini Musa, and Helena Manuel. «Optimization of microgrid operations using renewable energy sources». In: *Engineering Science & Technology Journal* 5 (July 2024), pp. 2379–2401. DOI: 10.51594/estj.v5i7.1360 (cit. on p. 8).

[12] Ghazanfar Shahgholian. «A brief review on microgrids: Operation, applications, modeling, and control». In: *International Transactions on Electrical Energy Systems* 31.6 (2021), e12885. DOI: https://doi.org/10.1002/2050-7038.12885. eprint: https://onlinelibrary.wiley.com/doi/pdf/10.1002/2050-7038.12885. URL: https://onlinelibrary.wiley.com/doi/abs/10.1002/2050-7038.12885 (cit. on p. 8).

[13] Ioannis Moschos, Ioannis Mastoras, and Parisses Constantinos. «A Potent Fractional-Order Controller for Interconnected Multi-Source Microgrids». In: *Electronics* 12 (Oct. 2023), p. 4152. DOI: 10.3390/electronics12194152 (cit. on p. 8).

[14] Xiaogang Dong, Jinqiang Gan, Hao Wu, Changchang Deng, Sisheng Liu, and Chaolong Song. «Self-Triggered Model Predictive Control of AC Microgrids with Physical and Communication State Constraints». In: *Energies* 15.3 (2022). ISSN: 1996-1073. DOI: 10.3390/en15031170. URL: https://www.mdpi.com/1996-1073/15/3/1170 (cit. on p. 9).

[15] Zhongqiang Wu and Hongqiang Cheng. «Voltage and Frequency Control of Microgrids Considering State Constraints and Attacks». In: *IEEE Transactions on Network Science and Engineering* 11.5 (2024), pp. 4979–4989. DOI: 10.1109/TNSE.2024.3410180 (cit. on p. 9).

[16] Hoummadi Mohammed Amine, Manale Bouderbala, Alami Hala, Badre Bossoufi, Najib El Ouanjli, and Mohammed Karim. «Survey of Sustainable Energy Sources for Microgrid Energy Management: A Review». In: *Energies* 18 (Mar. 2023), p. 17. DOI: 10.3390/en16073077 (cit. on p. 9).

[17] International Renewable Energy Agency (IRENA). *Renewable Energy Statistics 2024*. Abu Dhabi: International Renewable Energy Agency, 2024 (cit. on pp. 9, 10).

[18] Xiugao Pei, Xinhua Zhao, Huiyong Jia, Hao Wang, and Junpeng Liu. «Fuzzy sliding mode control with adaptive exponential reaching law for inverters in the photovoltaic microgrid». In: *Frontiers in Energy Research* 12 (June 2024). DOI: 10.3389/fenrg.2024.1416863 (cit. on p. 9).

[19] ShuMing Wang, XiaoHui Yuan, Qian Huang, AnQing Chen, HanBin Ma, and Xiang Xu. «Daily consumption monitoring method of photovoltaic microgrid based on genetic wavelet neural network». In: *International Journal of Low-Carbon Technologies* 18 (Mar. 2023), pp. 167–174. DOI: 10.1093/ijlct/ctac141 (cit. on p. 9).

[20] Plamen Stanchev, Gergana Vacheva, and Nikolay Hinov. «Evaluation of Voltage Stability in Microgrid-Tied Photovoltaic Systems». In: *Energies* 16 (June 2023), p. 4895. DOI: 10.3390/en16134895 (cit. on p. 9).

[21] International Renewable Energy Agency (IRENA). *Future of Solar Photovoltaic: Deployment, Investment, Technology, Grid Integration and Socio-economic Aspects*. A Global Energy Transformation: Paper. Abu Dhabi: International Renewable Energy Agency, 2019 (cit. on p. 9).

[22] International Renewable Energy Agency (IRENA). *Global Energy Transformation: A Roadmap to 2050 (2019 edition)*. Abu Dhabi: International Renewable Energy Agency, 2019 (cit. on p. 10).

[23] Dzisi Gadze, Sylvester Aboagye, and Kwame Agyekum. «Real Time Traffic Base Station Power Consumption Model for Telcos in Ghana». In: Aug. 2016 (cit. on p. 10).

[24] Gunther Auer et al. «How much energy is needed to run a wireless network?» In: *IEEE Wireless Communications* 18.5 (2011), pp. 40–49. DOI: 10.1109/MWC.2011.6056691 (cit. on p. 10).

[25] Nicola Piovesan, David Lopez-Perez, Antonio Domenico, Xinli Geng, and Harvey Bao. *Power Consumption Modeling of 5G Multi-Carrier Base Stations: A Machine Learning Approach*. Dec. 2022 (cit. on p. 12).

[26] M. Matalatala, M. Deruyck, E. Tanghe, L. Martens, and W. Joseph. «Simulations of beamforming performance and energy efficiency for 5G mm-wave cellular networks». In: *2018 IEEE Wireless Communications and Networking Conference (WCNC)*. IEEE, 2018, pp. 1–6 (cit. on p. 12).

[27] https://pvwatts.nrel.gov/pvwatts.php (cit. on pp. 12, 15).

[28] A. P. Dobos. *PVWatts Version 5 Manual*. Tech. Rep. Golden, CO (United States): National Renewable Energy Lab. (NREL), 2014 (cit. on pp. 13, 15).

[29] Richard Perez, Pierre Ineichen, Robert Seals, Joseph Michalsky, and Ronald Stewart. «Modeling daylight availability and irradiance components from direct and global irradiance». In: *Solar Energy* 44.5 (1990), pp. 271–289. ISSN: 0038-092X. DOI: https://doi.org/10.1016/0038-092X(90)90055-H. URL: https://www.sciencedirect.com/science/article/pii/0038092X9090055H (cit. on p. 13).

[30] Fuentes. «A simplified thermal model for Flat-Plate photovoltaic arrays». In: 1987. URL: https://api.semanticscholar.org/CorpusID:108123108 (cit. on p. 13).

[31] AGCOM - Autorità per le Garanzie Nelle Comunicazioni. *OSSERVATORIO SULLE COMUNICAZIONI N.4/2018*. Tech. rep. N.4/2018. Tech. Rep. N.4/2018. AGCOM - Autorità per le Garanzie Nelle Comunicazioni, 2018 (cit. on p. 15).

[32] «Simulations of beamforming performance and energy efficiency for 5 mm-wave cellular networks». In: *2018 IEEE Wireless Communications and Networking Conference (WCNC)*. IEEE, 2018, pp. 1–6 (cit. on p. 16).

[33] G. Vallero, E. Pristeri, and M. Meo. «Coping with power outages in mobile networks». In: *2020 Mediterranean Communication and Computer Networking Conference (MedComNet)*. IEEE, 2020, pp. 1–4 (cit. on p. 16).

Acknowledgements

This thesis marks the end of not only my master's degree but also a two-year journey in which I learned a lot, and here I want to thank all the people without whom this would have not been possible.

First of all, I want to thank Professor Meo and Doctor Vallero for all the support they gave me during my thesis, and for all the knowledge they passed on to me, but also for giving me the possibility to grow by working by my own.

A great thank you goes to my family. To my parents, for believing in me even when I didn't. To my grandparents, because I know they are proud of me, even if they are not all here to tell me so. To my brother Federico, because, as he never stops reminding me, I am who I am (also) thanks to him, and to Matilde, for supporting me and being an example of dedication.

Then, I want to thank all my friends who accompanied me on this journey. To Giacomo and Francesca, for being there even if we were no more in the same city. To Federico, Alessandro, Giovanni, and Davide, for sharing this adventure with me. To Elena, Chiara, and Matteo, for not letting me starve every day. And lastly, to Veronica and Elena, without whom this journey would not have been the same.